OPTICAL BIREFRINGENCE INDUCED BY SHEAR WAVE PROPAGATION IN AQUEOUS MILLING YELLOW SOLUTIONS

By

LOGAN E. HARGROVE, JR.

Bachelor of Science

Oklahoma Agricultural and Mechanical College

Stillwater, Oklahoma

1956

Submitted to the faculty of the Graduate School of
the Oklahoma State University in partial
fulfillment of the requirements
for the degree of
MASTER OF SCIENCE
August, 1957

OPTICAL BIREFRINGENCE INDUCED BY SHEAR WAVE PROPAGATION IN AQUEOUS MILLING YELLOW SOLUTIONS

Thesis Approved:

G. B. Thurston
Thesis Adviser

W. J. Lewis

Dean of the Graduate School

PREFACE

The optical interference patterns observed in a flow-birefringent fluid when viewed between crossed plane-polarizing plates are related to the fluid motion. Previous studies of this relation have been made using steady fluid flow conditions for which analytical solutions are available. The results have been used to study two-dimensional, steady, laminar flow conditions for which analytical solutions are not available.

The present work is a study of the observed optical interference patterns and a wave of transverse fluid vibrations propagating from the surface of an oscillating plane immersed in a flow-birefringent fluid. The fluid is an aqueous solution of milling yellow dye, a commercial dye product of the National Aniline Division of the Allied Chemical and Dye Corporation. The principal emphasis is placed on the relationship between the wave properties of the observed patterns and the wave of transverse fluid vibrations. This work is among the first done with flow-birefringence and unsteady (sinusoidal) fluid motion viewed specifically as a wave propagation problem.

Indebtedness is acknowledged to Dr. George B. Thurston for his valuable guidance as research and thesis adviser; and to the faculty and staff of the Department of Physics for their assistance; and to the Special Services Department of the Library for assistance in securing literature; and to the Office of Ordnance Research of the United States Army and the Research Foundation of the Oklahoma Agricultural and Mechanical College, without whose support this study would not have been possible.

TABLE OF CONTENTS

LIST OF FIGURES

CHAPTER I

INTRODUCTION

The optical interference patterns observed with a flow-birefringent fluid when viewed between crossed plane-polarizing plates are related to the fluid motion. Studies of this relation have been made by previous investigators. The bulk of these studies has been made using steady fluid flow conditions for which analytical solutions are available. Results have been used to study two-dimensional, steady, laminar flow conditions for which analytical solutions are not available.

As early as 1866[1] Maxwell made attempts to ascertain whether the state of strain in a viscous fluid might be detected by its action on polarized light. In 1873 he described an experiment with Canada balsam. The fluid was observed between crossed Nicol prisms while a flat spatula was moved up and down in the fluid. The appearance of light on both sides of the spatula, only so long as the spatula was in motion, was reported. Maxwell stated that he was not aware that this method of rendering visible the state of strain of a viscous fluid had hitherto been employed, and suggested it appears capable of furnishing important information.

Use of a flow-birefringent fluid for analysis of fluid motion was

---

[1] J. C. Maxwell, "On Double Refraction in a Viscous Fluid in Motion", Proc. Roy. Soc., 22, 46-47 (1873).

described by Humphry[2] in 1923. Some qualitative results were obtained using a vanadium pentoxide sol. In 1935 Alcock and Sadron[3] calculated local velocity gradients from measured values of double refraction in sesame oil and suggested further applications. Hauser and Dewey[4] reported on experiments in progress in 1939. Bentonite sols were used. In 1941, Dewey[5] gave the results in a thesis. Methods for quantitative calculations of local velocity gradients and streamline directions were given. Flow facility description, calibration data, and photographs of flow patterns were also presented. A similar analysis was presented by Weller[6, 7] in 1942. Some fifty liquids were tried.

In 1952 a summary and extension of the work of Dewey and Weller was presented by Rosenberg.[8] A survey of literature pertaining to flow-birefringence was also presented. Balint[9], in 1953, reviewed methods of

---

[2]R. H. Humphry, "Demonstrations of the Double Refraction Due to Motion of a Vanadium Pentoxide Sol and Some Applications", Proc. Roy. Soc. (London), 35, 217-218 (1923).

[3]E. D. Alcock and C. D. Sadron, "An Optical Method for Measuring the Distribution of Velocity Gradients in a Two-Dimensional Flow", Physics, 6, 92-95 (1935).

[4]E. A. Hauser and D. R. Dewey, "Study of Liquid Flow", Ind. Eng. Chem., 31, 786 (1939).

[5]D. R. Dewey, "Visual Studies of Fluid Flow Patterns Resulting From Streaming Double Refraction", Unpublished Doctoral Dissertation, Massachusetts Institute of Technology, 1941.

[6]R. Weller, J. J. Middlehurst, and R. Steiner, "The Photoviscous Properties of Fluids", NACA Tech. Note No. 841 (1942).

[7]R. Weller, "The Optical Investigation of Fluid Flow", J. App. Mech., 14, 103-107 (1947).

[8]B. Rosenberg, "The Use of Doubly Refracting Solutions in the Investigation of Fluid Flow Phenomena", Navy Dept. David W. Taylor Model Basin, Washington 7, D. C., Report No. 617, 1952.

[9]E. Balint, "Techniques of Flow Visualization", Aircraft Engineering, 25, 161-167 (1953).

flow visualization.

In 1953 it was found that aqueous solutions of milling yellow dye exhibit flow-birefringence. Milling yellow dye is a product of National Aniline Division of Allied Chemical and Dye Corporation, 3355 West 48th Place, Chicago 32, Illinois. A brief description of the flow-birefringence of aqueous solutions of milling yellow dye was presented by Peebles, Garber, and Jury.[10] They outlined future quantitative experiments using the dye. Office of Naval Research Contract Nonr-811(04) reports[11, 12, 13] describe determination of flow double refraction and rheological properties of aqueous solutions of milling yellow dye.

In 1954, Hargrove and Thurston[14] became interested in using aqueous milling yellow solutions to facilitate a study of fluid motion in the

---

[10] F. N. Peebles, H. J. Garber, and S. H. Jury, "Preliminary Studies of Flow Phenomena Utilizing a Double Refracting Liquid", Proc. Third Midwestern Conference on Fluid Mechanics, Minneapolis; The University of Minnesota Press, 1953.

[11] F. N. Peebles, J. W. Prados, and E. H. Honeycutt, Jr., "A Study of Laminar Flow Phenomena Utilizing a Double Refracting Liquid", Progress Report 1 under Contract No. Nonr-811(04), Knoxville, Tennessee, Engineering Experiment Station and Department of Chemical Engineering of the University of Tennessee (1954).

[12] J. W. Prados and F. N. Peebles, "A Study of Laminar Flow Phenomena Utilizing a Double Refracting Liquid", Progress Report 2 "Determination of the Flow Double Refraction Properties of Aqueous Milling Yellow Dye Solutions", Published Master's Thesis under Contract No. Nonr-811(04), Knoxville, Tennessee, Engineering Experiment Station and Department of Chemical Engineering of the University of Tennessee (1955).

[13] E. H. Honeycutt, Jr. and F. N. Peebles, "A Study of Laminar Flow Phenomena Utilizing a Doubly Refracting Liquid", Progress Report 3 "Rheological Properties of Aqueous Solutions of Milling Yellow Dye", Published Master's Thesis under Contract No. Nonr-811(04), Knoxville, Tennessee, Engineering Experiment Station and Department of Chemical Engineering of the University of Tennessee (1955).

[14] L. E. Hargrove, Jr. and G. B. Thurston, "Photographic Method for Analysis of Fluid Motion", J. Acoust. Soc. Am., 29, 179 (A) (1957).

vicinity of an orifice. In this work, sinusoidal oscillation of the fluid in the orifice and sinusoidal oscillation with a steady flow compoment were considered. With such flow cases, the fluid motion is periodic. Furthermore, the fluid motion is neither two-dimensional nor entirely laminar. Investigation was initiated to determine the flow-optic relations for time varying fluid motion. It is with this investigation that the present work is concerned.

The solution to the problem of Stokes' oscillating plane represents a wave of transverse fluid vibrations propagating from a plane boundary. The present work is a study of the observed optical interference patterns and the wave of transverse fluid vibrations. The chief emphasis is placed on the relationship between the wave properties of the observed patterns and the wave of transverse fluid vibrations. This work is among the first[15] done with flow-birefringence and unsteady (sinusoidal) fluid motion viewed specifically as a wave propagation problem.

---

[15] J. D. Ferry, "Studies of Mechanical Properties of Substances of High Molecular Weight, I. A Photoelastic Method for Study of Transverse Vibrations in Gels", Rev. Sci. Inst., 12, 79-82 (1941).

CHAPTER II

THEORY

(a) The Flow-optic Relation

The optical theory of double refraction is presented in Appendix B. A general treatment of the subject of streaming birefringence and many references are found in a book by Eirich.[16] A fluid which exhibits the phenomenon of flow birefringence (also called flow double refraction and streaming birefringence) behaves optically no differently from other fluids when it is at rest. Light travels through the fluid with a velocity inversely proportional to the index of refraction. The index of refraction is independent of the direction of propagation of the light and the orientation of the plane of polarization. When the fluid at rest is viewed between crossed polarizing plates, the plane of polarization is unchanged during passage of light through the fluid and thus light transmitted by the first polarizer is extinguished by the second polarizer.

When a flow-birefringent fluid is in motion with internal stresses due to viscosity and velocity gradients, the optical properties of the fluid are changed. The velocity of propagation of light through the fluid

---

[16] F. R. Eirich, Rheology (Academic Press, Inc., New York, 1956), Vol. I, Chapter 15.

is no longer independent of the direction of propagation and the plane of polarization. The fluid is therefore temporarily optically anisotropic.

Consider a path of light propagation through the fluid. At any point on this path there are two mutually perpendicular directions along which the electric vector may point and for which the electric vector will undergo no rotation due to passage through the medium. However, the velocities of propagation associated with these two orientations of the electric vector differ. The velocity of propagation associated with orientation I is inversely proportional to the index of refraction n_I for this orientation. Similarly for the second orientation II the index of refraction is n_{II}. Should the electric vector have an orientation different from I and II, the medium will effectively resolve the vector into components along the directions I and II. The two resolved components will then propagate with velocities associated with n_I and n_{II}. Depending on the total path of propagation under these conditions, the light emerging from the medium may be plane polarized with the electric vector having its original direction, it may be plane polarized with the electric vector being at right angles to the original vector, or it may be elliptically polarized. The orientation of the electric vector entering the medium is established by the first polarizer. A second polarizer on the exit side of the medium and oriented at right angles to the first will then transmit in accordance with the degree of rotation produced by the medium.

In order to describe how a flow-birefringent fluid produces a pattern which is characteristic of a particular condition of fluid motion, consider the simple case of an element of moving fluid illuminated by parallel rays of light through crossed plane-polarizing plates. Refer to figure 1. When the plane polarized light with the electric vector oriented in a direction parallel to OX is transmitted by the first polarizer and then

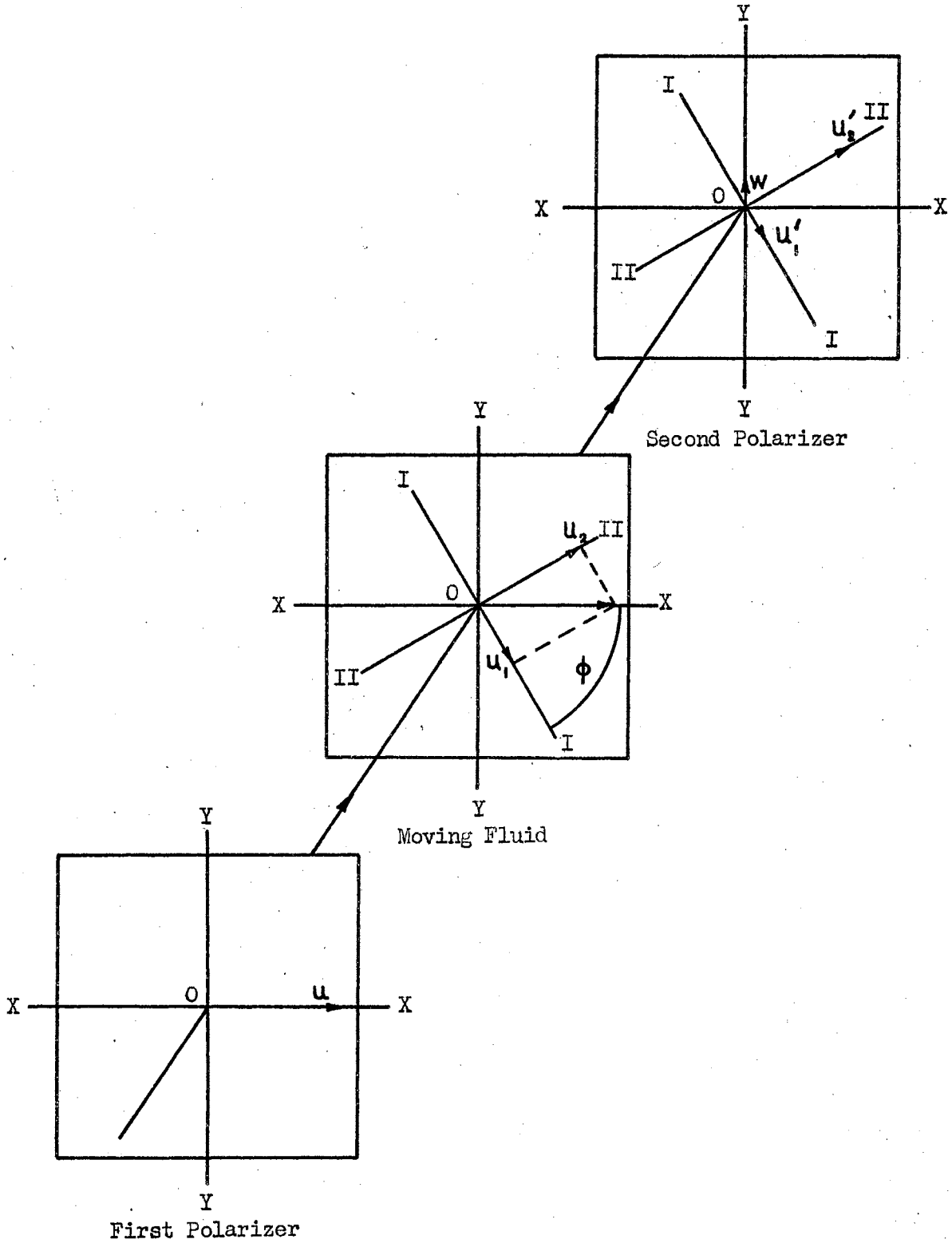

Figure 1. A schematic representation of plane polarized light passing through an element of flow-birefringent fluid.

passes through the flow-birefringent fluid, it is broken into two plane polarized components directed along directions I and II. If the equation for the plane polarized light is expressed as a function of time by

$$u = a \, \text{SIN} \frac{2\pi}{\lambda} (ct - x) \tag{2.1}$$

where

u = electric vector

a = amplitude

λ = wavelength

X = arbitrary phase retardation indicating that the electric vector is not necessarily zero at $t = 0$

C = velocity of light in vacuo,

then the equations for the components I and II respectively, for light entering the flow-birefringent fluid, are

$$u_1 = a \, \text{COS} \, \phi \, \text{SIN} \frac{2\pi}{\lambda} (ct - x) \tag{2.2}$$

and

$$u_2 = a \, \text{SIN} \, \phi \, \text{SIN} \frac{2\pi}{\lambda} (ct - x) \tag{2.3}$$

where

u_1 = component of the electric vector in the direction I

u_2 = component of the electric vector in the direction II

ϕ = angle made by I with OX.

Since the two components u_1 and u_2 do not travel at the same velocity

through the flow-birefringent fluid, the slower will emerge some distance δ behind the faster. This relative retardation can be expressed quantitatively by the equations for the light leaving the fluid as

$$u_1' = a \cos\phi \sin\frac{2\pi}{\lambda}(ct - x) \tag{2.4}$$

and

$$u_2' = a \sin\phi \sin\frac{2\pi}{\lambda}(ct - x - \delta) \tag{2.5}$$

where

u_1' = component of the electric vector direction I, leaving the flow-birefringent fluid

u_2' = component of the electric vector direction II, leaving the flow-birefringent fluid

δ = relative retardation produced by passage through the flow-birefringent fluid.

When u_1' and u_2' reach the second polarizer, only the component of the electric vector parallel to OY is transmitted. Thus the equation for the light transmitted through the second polarizer can be expressed as a resultant obtained by adding the components of u_1' and u_2' parallel to OY. This resultant W is given by

$$W = u_1' \sin\phi - u_2' \cos\phi. \tag{2.6}$$

Combining the values of u_1' and u_2' given in equations (2.4) and (2.5) with equation (2.6) and simplifying gives

$$W = \left[a \sin 2\phi \sin \frac{\pi\delta}{\lambda} \right] \cos \frac{2\pi}{\lambda}(ct - x - \frac{\delta}{2}) \qquad (2.7)$$

where $\left[a \sin 2\phi \sin \frac{\pi\delta}{\lambda} \right]$ represents the amplitude of the resultant electric vector. Equation (2.7), giving the final resultant electric vector W which is passed by the second polarizer, indicates the conditions for existance of points of zero light intensity. Since the intensity of the transmitted light is proportional to the square of the amplitude, zero intensity requires that

$$\left[a \sin 2\phi \sin \frac{\pi\delta}{\lambda} \right]^2 = 0. \qquad (2.8)$$

This requirement is satisfied for

$$2\phi = N\pi \qquad (2.9)$$

and

$$\frac{\pi\delta}{\lambda} = N\pi \qquad (2.10)$$

or, expressed in terms of ϕ and δ,

$$\phi = \frac{N\pi}{2} \qquad (2.11)$$

and

$$\delta = N\lambda \qquad (2.12)$$

where N is zero or an integer. These relations indicate that zero resultant intensity occurs where

(1) direction I is oriented at an angle $\phi = \frac{N\pi}{2}$ with respect to

the transmission direction OX of the first polarizer, or

(2) the relative retardation δ produced by the passage of plane polarized light through the flow-birefringent fluid is a distance equal to an integral number of wavelengths of the incident light.

Consider the second condition for zero resultant intensity of light transmitted by the second polarizer. The velocities of the component rays are given by

$$C_{II} = C / n_{II} \tag{2.13}$$

and

$$C_{I} = C / n_{I} . \tag{2.14}$$

If $n_I > n_{II}$ component I will be slowed behind component II and will emerge from the fluid element a small time interval after component II. This time interval is

$$\Delta t = \frac{S}{C/n_I} - \frac{S}{C/n_{II}} = \frac{S}{C}(n_I - n_{II}) \tag{2.15}$$

where

Δt = time interval between the emergence of components II and I

S = length of the light path through the fluid element.

Since both components travel in air with a velocity approximately equal to the velocity of light in vacuo, I will be retarded behind II by a distance δ given by

$$\delta = C \Delta t = S(n_I - n_{II}). \tag{2.16}$$

The factor $(n_I - n_{II})$ is called the amount of birefringence.

It is reported in page 616 of reference 17 that

$$(n_I - n_{II}) = f\left[\frac{\partial \dot{\xi}}{\partial \bar{n}}\right] \tag{2.17}$$

where f is a functional notation, $\dot{\xi}$ is the fluid velocity, and $\bar{n}$ is in the direction normal to the plane flow lamina. Thus from equation (2.16), the relative retardation δ is given by

$$\delta = Sf\left[\frac{\partial \dot{\xi}}{\partial \bar{n}}\right]. \tag{2.18}$$

Furthermore,

$$f[0] = 0. \tag{2.19}$$

Equations (2.18) and (2.19) shall be called the flow-optic relation.

For plane laminar fluid motion, the stress in a viscous fluid is given by

$$\text{shearing stress} = \mu \frac{\partial \dot{\xi}}{\partial \bar{n}} \tag{2.20}$$

where μ is the fluid viscosity. This suggests that the optical effects may be related to the stresses in the fluid. Discussion of stress dependence of birefringence is presented in Appendix B.

(b) Stokes' Oscillating Plane

Consider the classical hydrodynamic problem known as Stokes' oscillating plane.[17] Refer to figure 2. A plane, infinite in extent in the

[17] H. Lamb, Hydrodynamics (Dover Publications, Inc., New York, 1932), pp. 619-621.

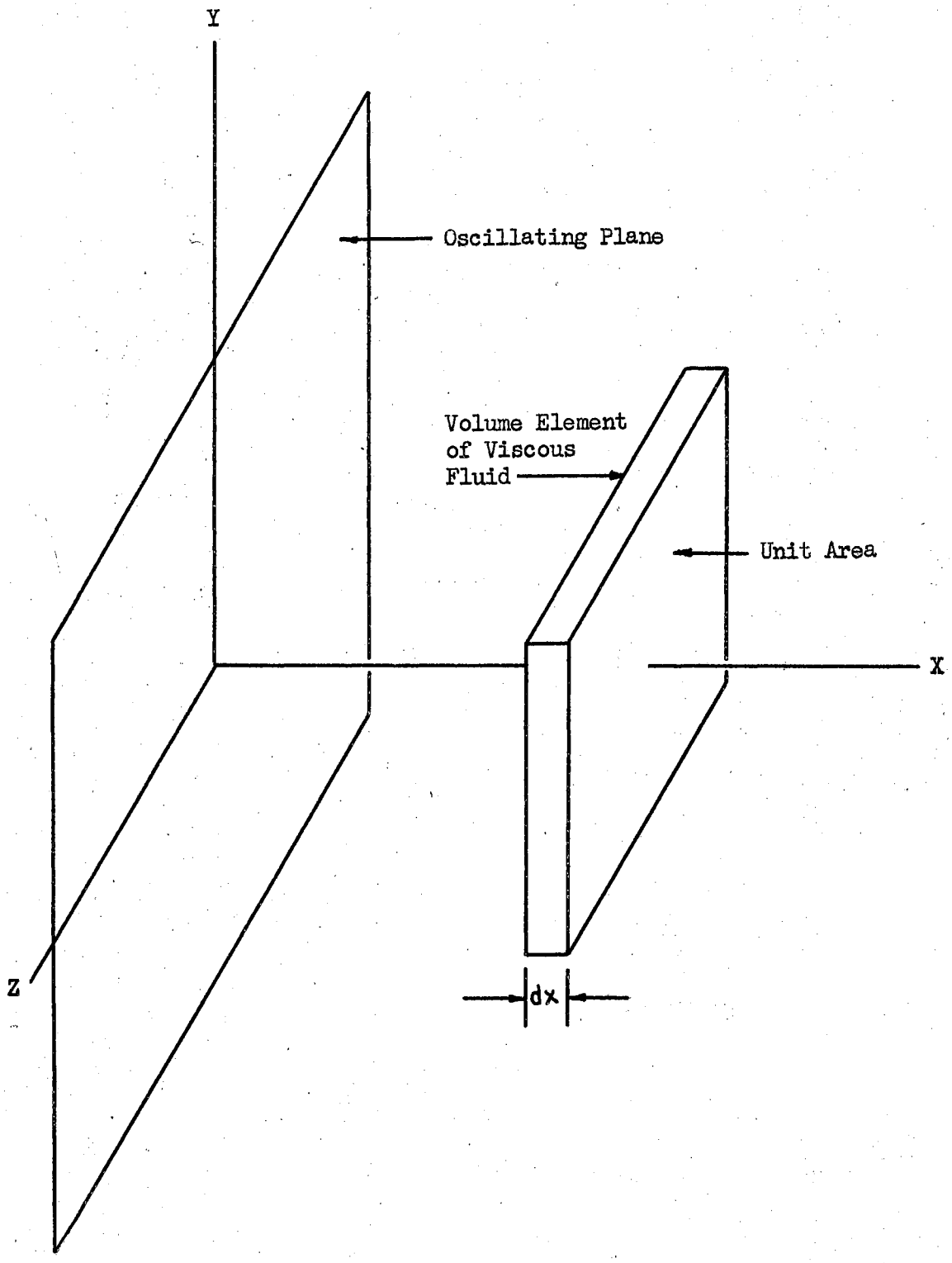

Figure 2. A pictorial representation of a finite section of Stokes' oscillating plane, a plane of infinite extent immersed in a viscous fluid and oscillating in its own plane. A volume element with unit area in the Y-Z plane is shown.

Y and Z directions, oscillates in its own plane in the Y direction. Let the plane be immersed in a viscous fluid, and describe the motion of the plane by

$$\dot{\xi} = \dot{\xi}_o \exp[i\omega t] \tag{2.21}$$

where

$\dot{\xi}$ = velocity in the Y direction

$\dot{\xi}_o$ = peak velocity amplitude of the plane

$i = (-1)^{1/2}$

ω = angular frequency of oscillation

t = time.

Consider the forces acting on a volume element having unit area in the Y-Z plane. The inertial force on the volume element is

$$f_i = ma = \rho dX \ddot{\xi} \tag{2.22}$$

where

f_i = inertial force

m = mass

a = acceleration

ρ = fluid density

dX = thickness of volume element in X direction

$\ddot{\xi}$ = second time derivative of displacement in Y direction.

The shear force acting on the volume element is

$$f_s = \frac{\partial}{\partial X}\left(\mu \frac{\partial \dot{\xi}}{\partial X}\right) dX \tag{2.23}$$

where

f_s = shear force

μ = coefficient of viscosity.

Equating the forces given in equations (2.21) and (2.23) and simplifying results gives the partial differential equation

$$\mu \frac{\partial^2 \dot{\xi}}{\partial x^2} = \rho \frac{\partial \dot{\xi}}{\partial t} \tag{2.24}$$

where μ is considered a constant. Assume the fluid does not slip at the plane surface and thus is moving in the same manner as the plane. A solution may be assumed to be of the form

$$\dot{\xi} = \dot{\xi}_0 \exp\left[i(\omega t - Kx)\right] \tag{2.25}$$

where K is a constant to be evaluated. Substitution of $\dot{\xi}$ from equation (2.25) into equation (2.24) gives

$$\mu \frac{\partial^2}{\partial x^2}\left\{\dot{\xi}_0 \exp\left[i(\omega t - Kx)\right]\right\} = \rho \frac{\partial}{\partial t}\left\{\dot{\xi}_0 \exp\left[i(\omega t - Kx)\right]\right\} \tag{2.26}$$

or

$$-\mu \dot{\xi}_0 K^2 \exp\left[i(\omega t - Kx)\right] = i\rho \dot{\xi}_0 \omega \exp\left[i(\omega t - Kx)\right] \tag{2.27}$$

giving

$$K^2 = -\frac{i\omega\rho}{\mu}. \tag{2.28}$$

Since $(-i)^{1/2} = (1-i)/(2)^{1/2}$, K is given by

$$K = \left(\frac{\rho\omega}{2\mu}\right)^{1/2} - i\left(\frac{\rho\omega}{2\mu}\right)^{1/2}. \tag{2.29}$$

Having evaluated K , replacing K in equation (2.25) gives

$$\dot{\xi} = \dot{\xi}_0 \exp\left\{-\left(\frac{\omega\rho}{2\mu}\right)^{1/2} X\right\} \exp\left\{i\left[\omega t - \left(\frac{\omega\rho}{2\mu}\right)^{1/2} X\right]\right\} . \tag{2.30}$$

Equation (2.30) has the form

$$\dot{\xi} = \dot{\xi}_0 \exp\left[-\frac{2\pi X}{\lambda}\right] \exp\left[i\left(\omega t - \frac{2\pi X}{\lambda}\right)\right] \tag{2.31}$$

where λ is the viscous wavelength, and represents a wave of transverse fluid vibrations propagated from the plane surface. The viscous wavelength is given by

$$\lambda = 2\pi\left(\frac{2\mu}{\rho\omega}\right)^{1/2} . \tag{2.32}$$

and since $V = \frac{\lambda\omega}{2\pi}$ where V is the velocity of propagation of the wave then

$$V = \left(\frac{2\mu\omega}{\rho}\right)^{1/2} . \tag{2.33}$$

The amplitude factor $\exp\left[\frac{2\pi X}{\lambda}\right]$ indicates a velocity amplitude attenuation of $\exp(-2\pi)$ per wavelength.

Let the equation of motion of the oscillating plane be

$$\dot{\xi} = \dot{\xi}_0 \, \mathrm{SIN}\, \omega t . \tag{2.34}$$

The corresponding form of the equation of motion for the viscous fluid becomes

$$\dot{\xi} = \dot{\xi}_0 \exp\left[-\frac{2\pi X}{\lambda}\right] \mathrm{SIN}\left(\omega t - \frac{2\pi X}{\lambda}\right) \tag{2.35}$$

where λ is given by equation (2.32). A plot of the function expressed by equation (2.35) is presented in figure 3.

Associated with the wave of transverse fluid vibration is a viscous shear wave, related to the velocity gradient by the fluid viscosity, as given in equation (2.20). Equation (2.20) becomes

$$\text{shearing stress} = \mu \frac{\partial \dot{\xi}}{\partial x} . \tag{2.36}$$

From equations (2.12), (2.18), (2.19), (2.32), (2.33), and (2.35), relations can be formulated between the optical phenomena and the viscous shear wave.

(c) The Flow-optic Relation and Stokes' Oscillating Plane

Consider the previously derived condition for zero resultant intensity of transmitted light given in equation (2.12). With monochromatic light the light will be completely extinguished for all light paths for which the relative retardation is zero or an integral number of wavelengths. The light will be partially transmitted in varying intensities for other light paths.

If, rather than monochromatic light, white light is used, a continuous range of wavelengths of light pass through the fluid. The transmission over this range will also depend on the inherent optical transmission of the undisturbed fluid. From point to point, the successive colors will be extinguished as the relative retardation equals an integral multiple of its own wavelength, the remaining colors being transmitted with varying intensities according to the nearness of the relative retardation to an integral multiple of their own wavelengths. However, for the special case $N = 0$, zero intensity will result for any wavelength, producing a zero

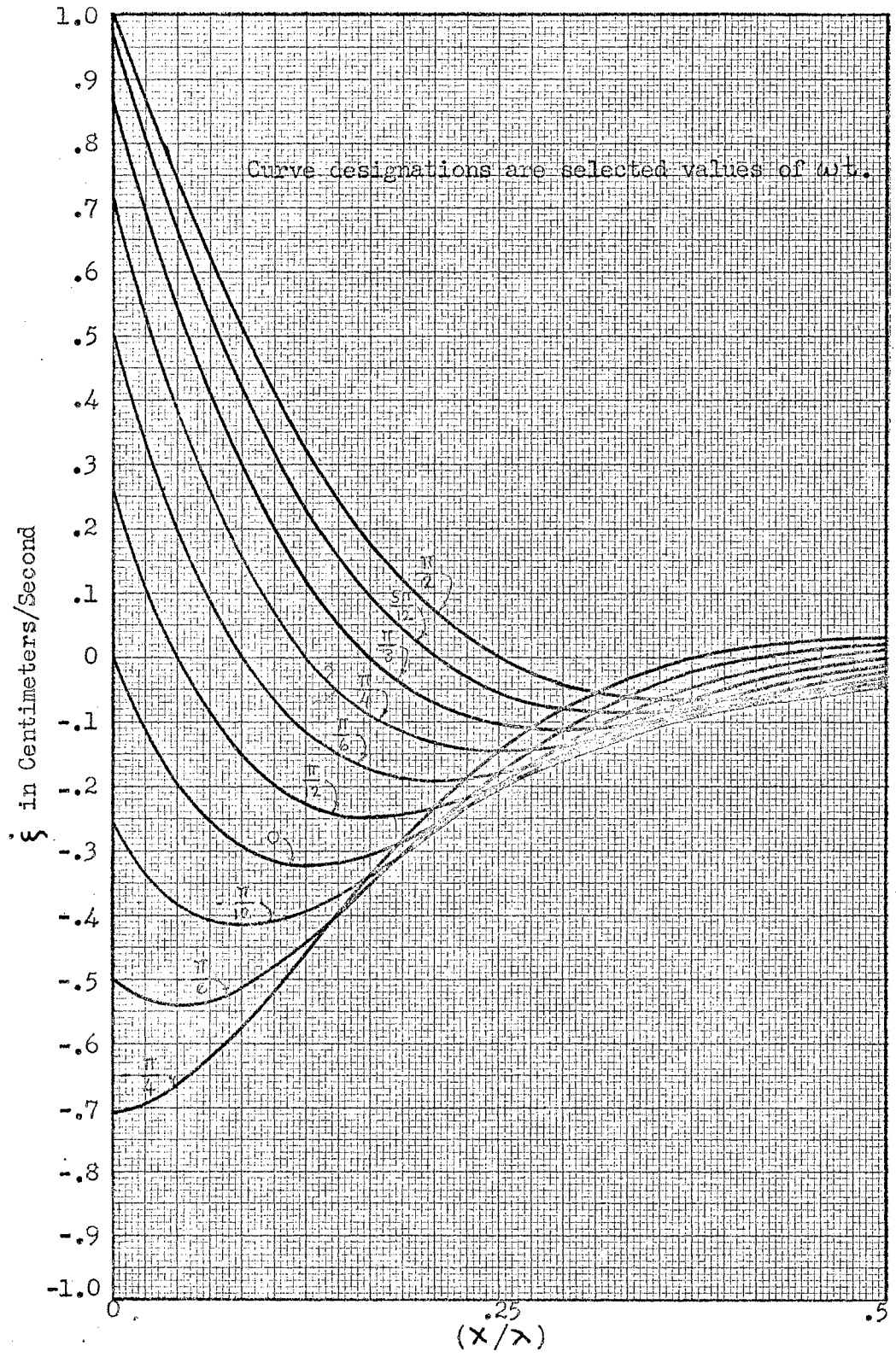

Figure 3. The function expressed by equation (2.35) versus (X/λ) for selected values of ωt. $\dot{\xi}_o$ is chosen equal to 1.0 cm/sec.

order fringe which can be identified in a field of higher order fringes by its characteristic lack of color. White light is used in the present work and primary consideration is given the zero order fringes.

Let the X-Y plane of figure 1 be coincident with that of figure 2. Then the light path O-O will be parallel to the Z axis in figure 2. Then for an infinite oscillating plane, the velocity gradient at points along the light path is uniform. Furthermore, the velocity gradients are in the X-Y plane only. Thus the thin section analysis as presented in figure 1 is applicable to a thick section in the neighborhood of an infinite oscillating plane.

Equations (2.18) and (2.19) indicate that $\delta = 0$ for $\frac{\partial \dot{\xi}}{\partial X} = 0$. A zero order fringe results for $\delta = 0$. If the optical effects are shear dependent, as discussed in Appendix B, equations (2.18) and (2.19) still give the condition for $\delta = 0$. This follows from the fact that if $\frac{\partial \dot{\xi}}{\partial X} = 0$ then the shear stress is zero. From equation (2.35)

$$\frac{\partial \dot{\xi}}{\partial X} = -(2)^{1/2} \dot{\xi}_o \frac{2\pi}{\lambda} \exp\left[-\frac{2\pi X}{\lambda}\right] \mathrm{SIN}\left(\omega t - \frac{2\pi X}{\lambda} + \frac{\pi}{4}\right). \quad (2.37)$$

For $\frac{\partial \dot{\xi}}{\partial X} = 0$ in equation (2.37)

$$\mathrm{SIN}\left(\omega t - \frac{2\pi X}{\lambda} + \frac{\pi}{4}\right) = 0 \quad (2.38)$$

from which the equation for propagation of zero order fringes from the plane surface becomes

$$X = Vt + \frac{\lambda}{8} \pm \frac{n\lambda}{2} \quad (2.39)$$

where n is an integer or zero and λ and ν are given by equations (2.32) and (2.33). Methods for measurement of zero order fringe propagation and related parameters are discussed in the following chapter.

CHAPTER III

EXPERIMENTAL METHODS

(a) The Experimental Apparatus

The experimental apparatus used in this study approximates Stokes' oscillating plane with a plane of finite dimensions. The flow facility and associated equipment is shown in simplified form in figure 4. A Plexiglas plastic plate 1/16 inch thick was caused to oscillate in its own plane. Plates of width varying from 5.12 cm to 0.64 cm in approximately 0.64 cm steps were used. Approximately 2 inches of the plate was immersed in the flow-birefringent fluid, an aqueous solution of milling yellow dye. The milling yellow solution was contained in a 1/4 inch Plexiglas plastic tank 2 inches by 2 inches by 4 inches deep, inside dimensions. The plate was driven sinusoidally, as required by equation (2.21), by a geophone type driver. The velocity of the plate was monitored and measured by the electrical output of an electrodynamic monitor. A common shaft connects the plate holder, geophone driver, and velocity monitor. The velocity monitor was calibrated from measurements of its electrical output and determinations of its excursion made with a traveling microscope under stroboscopic illumination. The velocity monitor output was measured with a Hewlett-Packard Model 400D vacuum tube voltmeter.

The driving energy for the system was provided by a Hewlett-Packard Model 200CD Wide Range Oscillator. The output of this oscillator was channeled through an attenuator to the geophone driver.

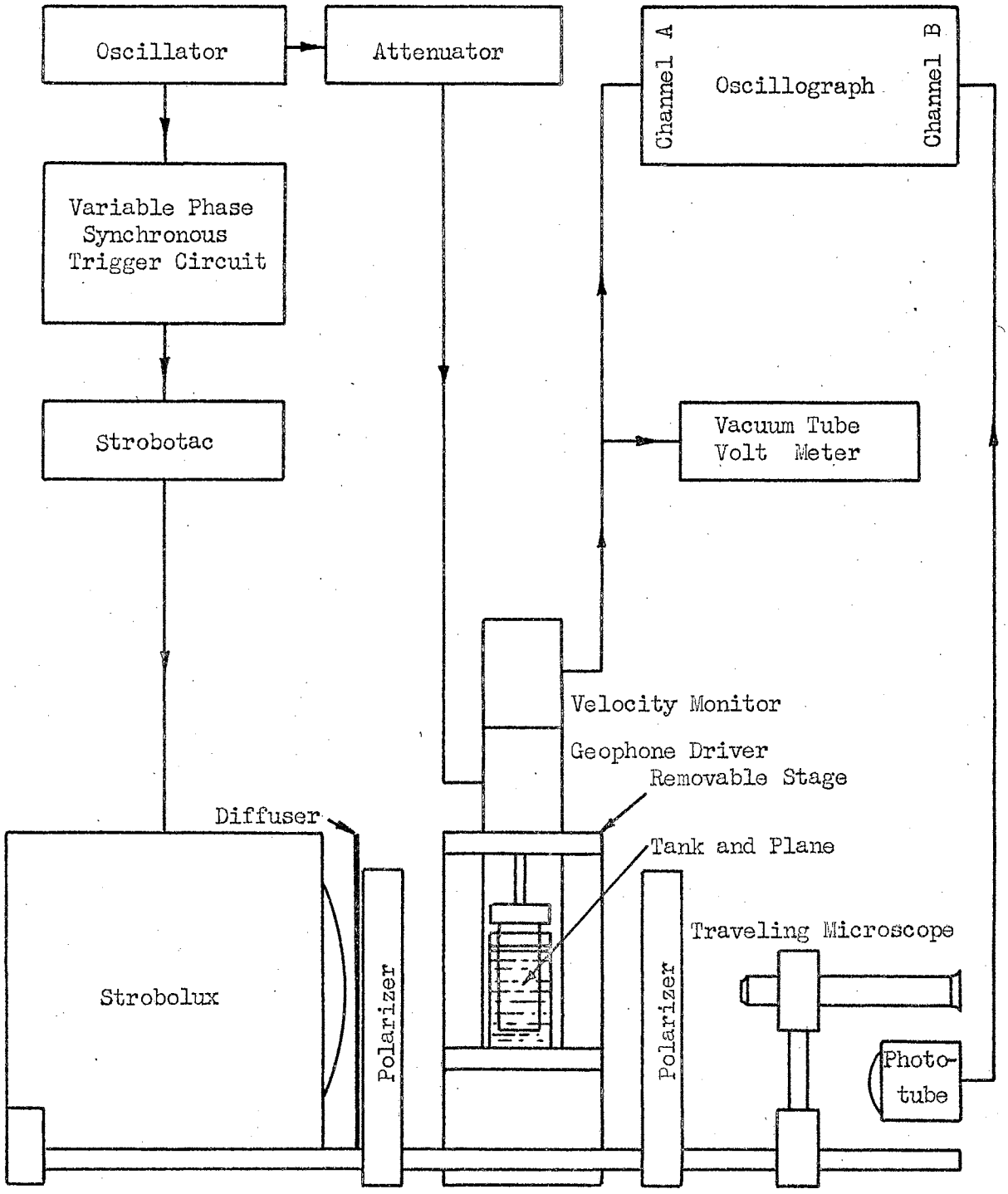

Figure 4. The flow facility and associated equipment in simplified form.

Stroboscopic illumination was furnished by a General Radio Type 648-A Strobolux. The Strobolux was triggered by a General Radio Type 631-A Strobotac, which could be externally controlled. To insure exact frequency synchronism of the light source with the oscillating plane, a circuit was provided to control the Strobotac externally with a pulse derived from a portion of the output of the oscillator which drives the plane. A variable phase shifting circuit was incorporated in the trigger circuit so that the observed phase of plane velocity could be varied. The schematic diagram of the variable phase synchronous trigger circuit is presented in figure 5.

A diffuser and polarizers are placed as shown in figure 4. A phototube pulse circuit, shown in figure 6, detects the flashing light from the Strobolux and produces an electrical pulse. The output of this pulse circuit and the output of the velocity monitor are presented on the separate channels of a Dumont Type 322-A Dual Beam Cathode Ray Oscillograph where they are swept with a common sweep generator. Determination of the observed phase of plane velocity was made graphically from enlarged photographs of the cathode ray oscillograph display, taken with a Dumont Type 296 Oscillograph-Record Camera. Phase determination was also made by visual inspection of the oscillograph display.

Measurements of fringe coordinates were made directly, using a Gaertner traveling microscope focused in the fluid. A short focal length microscope was fitted with a polarizer. When a long focal length microscope was used, a fixed polarizer was used. Zero order fringes are identified at small velocity amplitudes where they are more easily distinguished from higher order fringes. The traveling microscope cross-hairs are set on a zero order fringe and the fringe is observed while the velocity amplitude is slowly increased by adjustment of the driver attenuator.

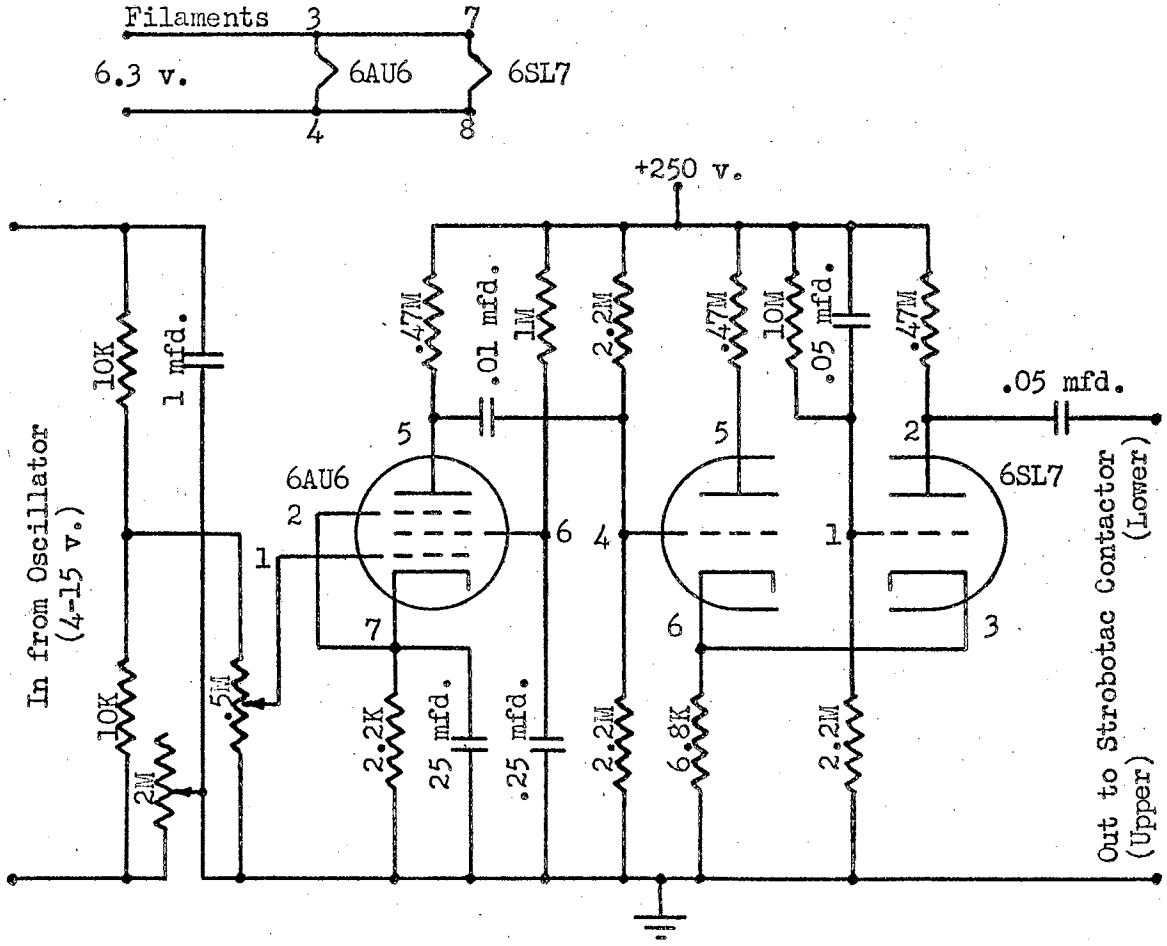

Figure 5. Schematic diagram of the variable phase synchronous trigger circuit used for external control of the Strobotac.

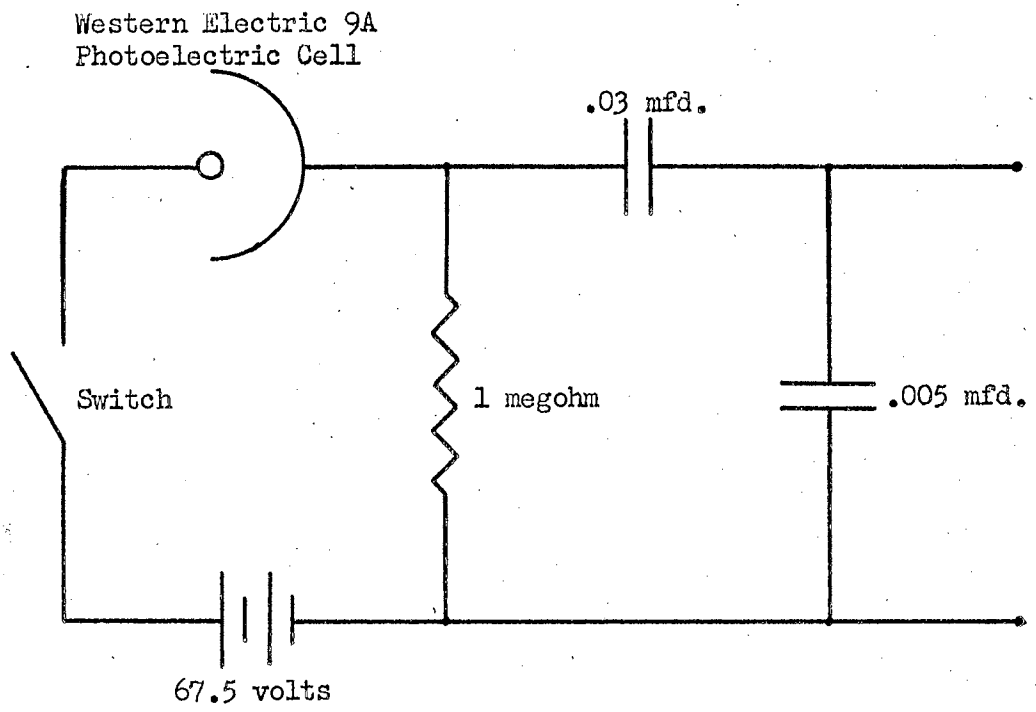

Figure 6. Schematic diagram of the photo-tube pulse circuit used to detect the Strobolux flash.

At the same time, the setting of the microscope is refined as the zero order fringe becomes narrow but less distinguishable from higher order fringes.

The main supporting structure of the apparatus, exclusive of associated electronic equipment, was a General Radio Type 1534-A Polariscope with some supplementary attachments. The geophone driver and velocity monitor were mounted on a removable stage above the tank.

(b) Milling Yellow Dye Solutions

It has been found[10, 11, 12, 13] that aqueous solutions of milling yellow dye in concentrations from 1.2 to 1.5% by weight are strongly birefringent. The viscosity is reported non-Newtonian, ranging from 1 to 200 centipoises, depending on dye concentration, temperature and shear-rate. The solutions are stable in contact with common materials.

Milling yellow dye, in dry powder form, is almost insoluble at room temperature. The dye material will go into solution at near boiling and will not precipitate when cooled. Solutions are prepared by mixing the necessary amount of dye material with approximately 20% excess distilled water and then heating the mixture to completely dissolve the dye material and evaporate excess water. After the solution is cooled, the concentration may be computed using the weight of dye material used and the weight of the final solution. An alternate method consists of drying a sample of know weight and then weighing the residue. This latter method is the more accurate of the two methods.

(c) Description and Analysis of the Experiment

The characteristics of the optical interference patterns observed in the vicinity of an oscillating plane are shown in figure 7. The

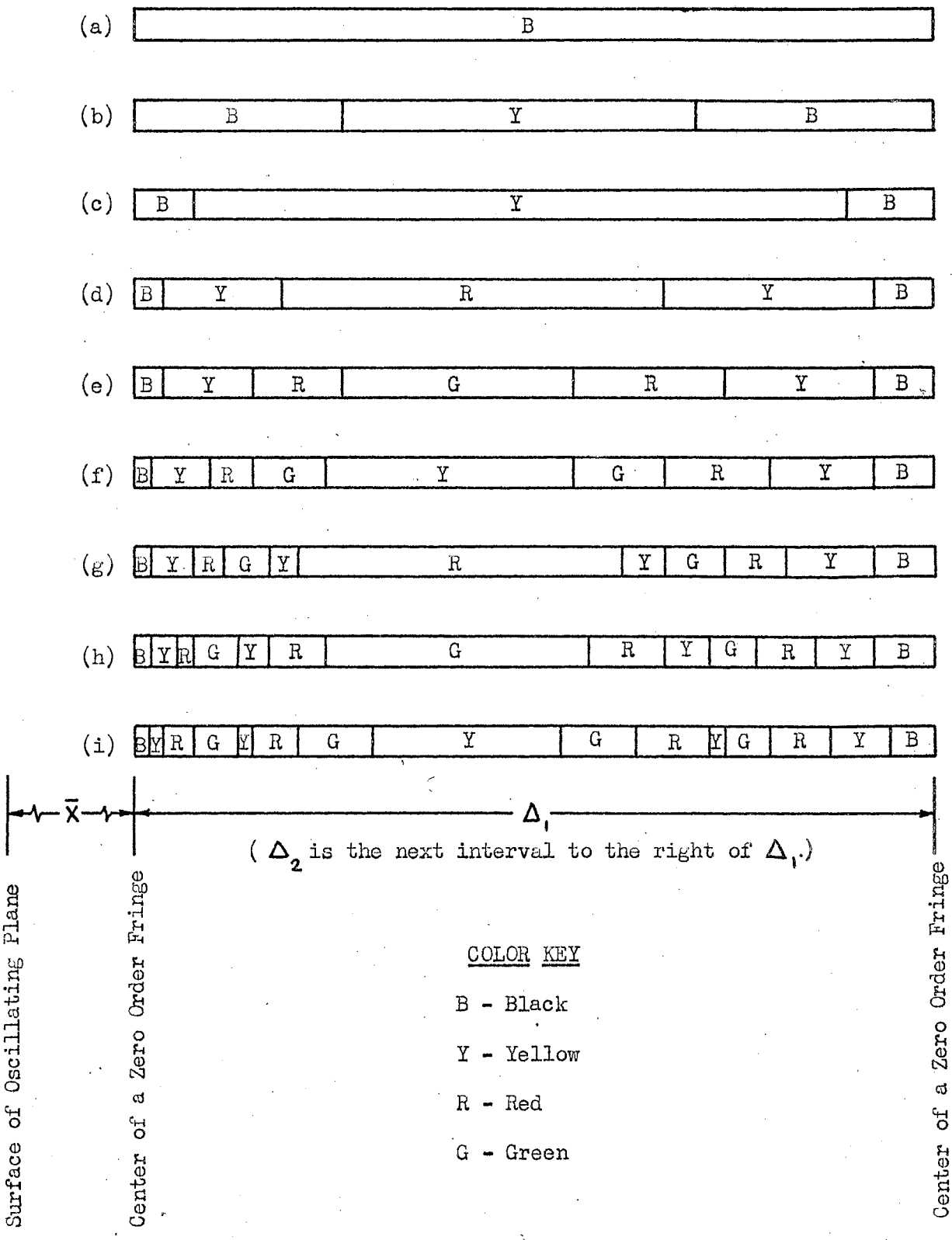

Figure 7. Characteristics of the optical interference patterns observed in the vicinity of an oscillating plane in a typical interval Δ . Also shown in the diagram are definitions of the symbols used in describing the experimentally measured parameters.

symbols used in describing the patterns are also explained in the figure. The separate horizontal strips represent typical patterns observed in an interval Δ and show the progression of the observed pattern as the velocity amplitude is increased. The particular case shown in figure 7 is for a 5.12 cm plane oscillating at 25 cps with peak velocity amplitudes from zero to 0.872 cm/sec in a 1.30% milling yellow solution. The observed plane velocity is positive maximum, where positive is taken as up. With further increase in velocity amplitude, colors continue to successively appear in the central section of the interval, appearing in the order yellow, red, and green. Blue is not observed in the patterns. Aqueous solutions of milling yellow dye do not transmit the blue portion of the spectrum. A plot of the optical transmittance of approximately 1.30% milling yellow solution is presented in figure 8. The per cent transmittance is taken with respect to air and was measured using a Model DK Beckman Recording Spectrophotometer.

When a new color band appears in the central section of the interval, the bands already present remain and "pack" against the black zero order fringes which define the interval. These observations are typical of any interval Δ . It will be noted that the patterns are not symmetric with respect to a line mid-way between the zero order fringes, but that the pattern is shifted in the direction of the oscillating plane. This is in general agreement with the fact that the amplitude at the midpoint of the interval is less than the average of the values at the extremes of the interval.

Experimental data were obtained in order to determine the effects of various parameters related to the geometry of the flow facility and optical system. Based on measurements of fringe coordinates, the error was analyzed with respect to

(1) plane width in the direction of the optical path

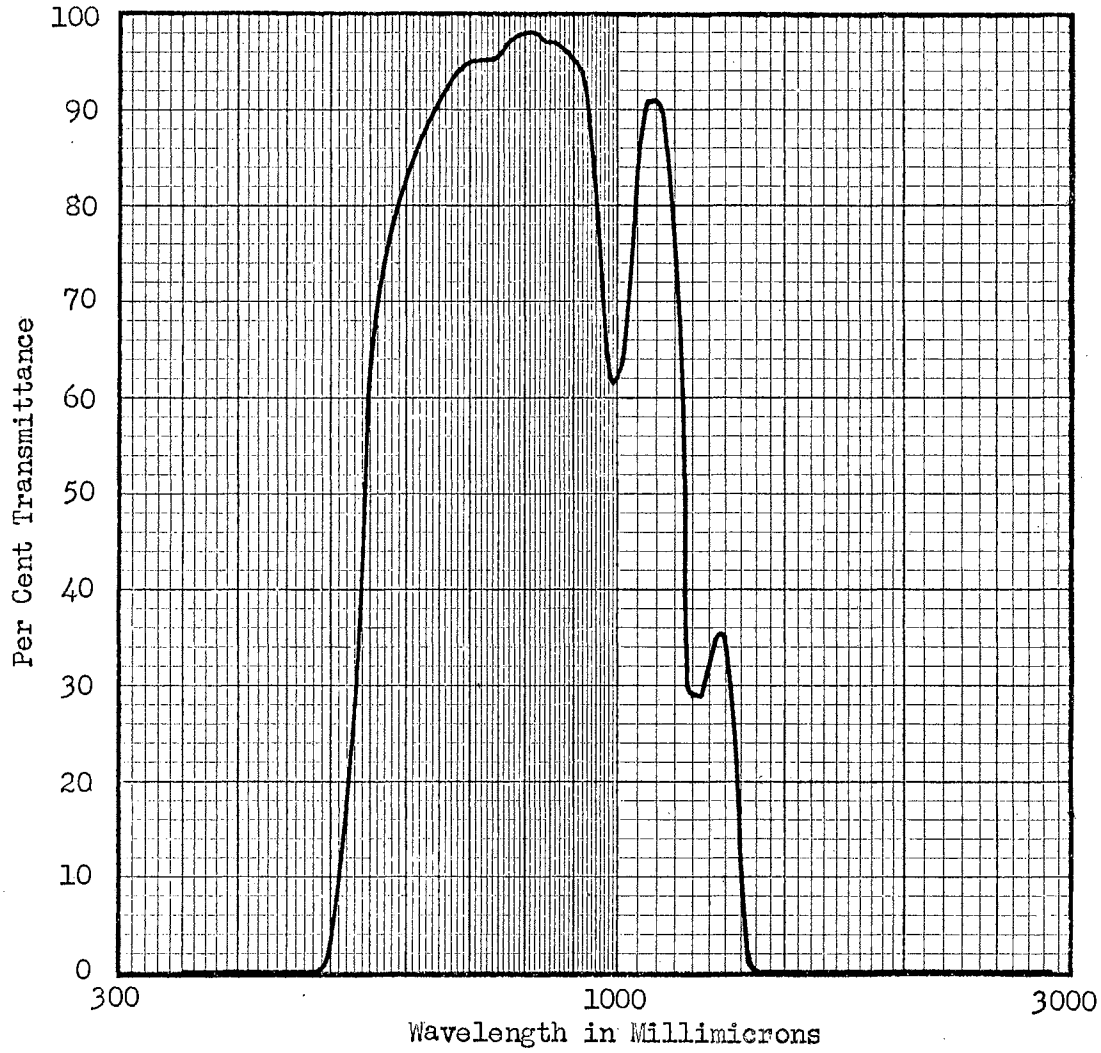

Figure 8. Optical transmittance with respect to air of 1.30% milling yellow solution as a function of wavelength of light.

(2) height of observation with respect to the bottom of the plane

(3) spacing between the plane and the tank wall

(4) alignment of the polaroids for extinction

(5) alignment of the plane, tank and microscope with respect to each other

(6) tilt of the oscillating plane so as not to oscillate in its own plane

(7) precision of reproduction of measurements.

To study the effect of varying the plane width, zero order fringe coordinates were measured for several plane widths. Results obtained for five different planes oscillating at 25 cps with a peak velocity amplitude of 1.745 cm/sec in a 1.30% milling yellow solution are presented in figure 9. The observed plane velocity is positive maximum. The deviations in Δ_1 represent ±3% of Δ_1. Similar deviations appear in $\Delta_1+\Delta_2$ and $\Delta_1+\Delta_2+\Delta_3$.

To determine the maximum distance from the plane for which a plane of finite extent approximates an infinite plane, Δ_1 as a function of $\bar{X}$ was determined for two successive Δ's. Figure 10 shows results obtained for a 2.56 cm plane oscillating at 25 cps with a peak velocity amplitude of 4.362 cm/sec in a 1.30% milling yellow solution. Figure 11 shows results obtained for a 5.12 cm plane oscillating with a peak velocity amplitude of 2.181 cm/sec. Slight temperature difference is responsible for the lack of internal consistancy in the data of figures 10 and 11. The deviations in the Δ's with increased distance from the plane for the narrower plane are more pronounced than for the wider plane. These results show that measurements using the 2.56 cm plane at 25 cps should be limited to $\bar{X} < 0.4$ cm and measurements using the 5.12 cm plane should be limited to $\bar{X} < 0.8$ cm for an acceptable approximation to an oscillating

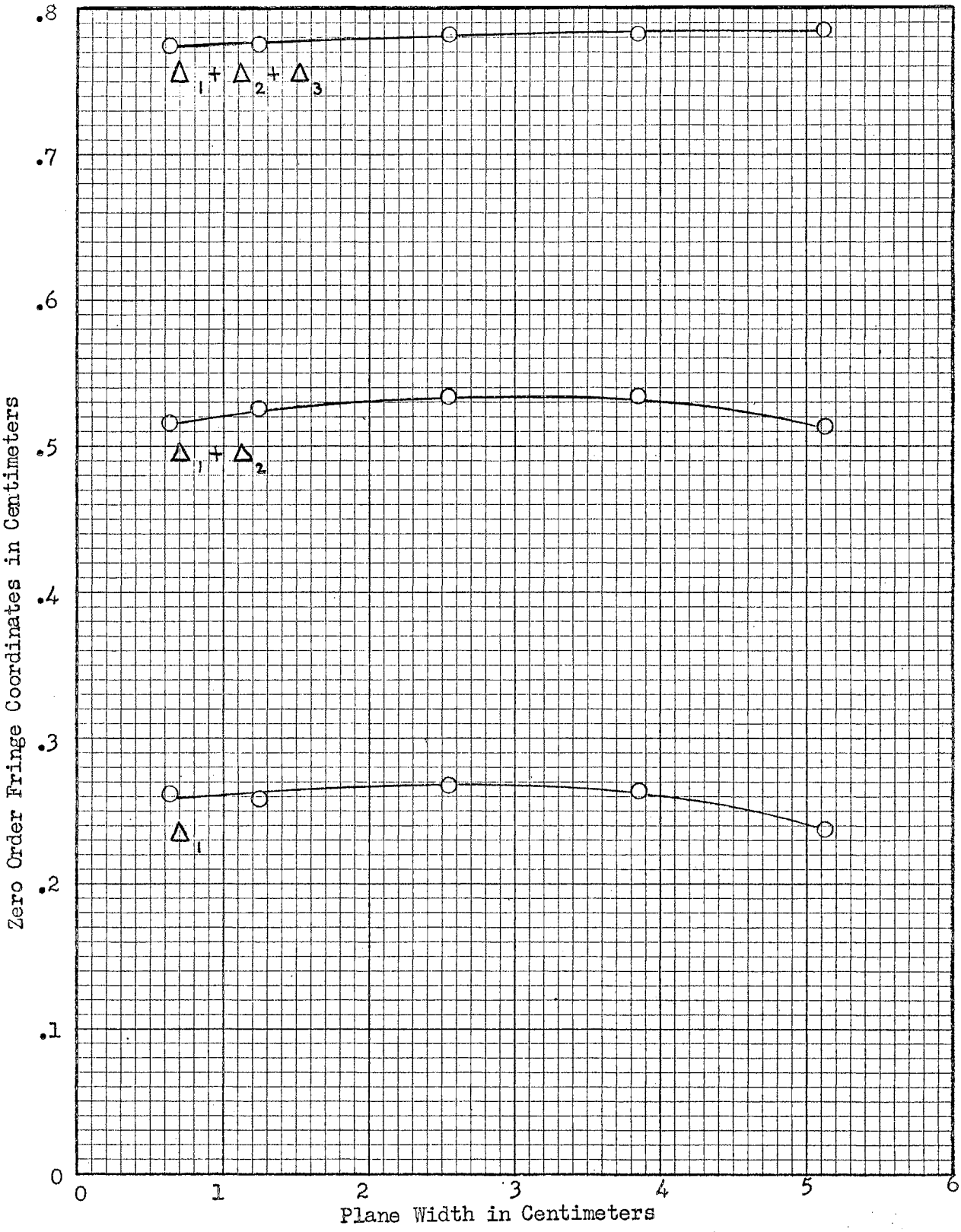

Figure 9. Zero order fringe coordinates as a function of plane width for planes oscillating at 25 cps with a peak velocity amplitude of 1.745 cm/sec in a 1.30% milling yellow solution.

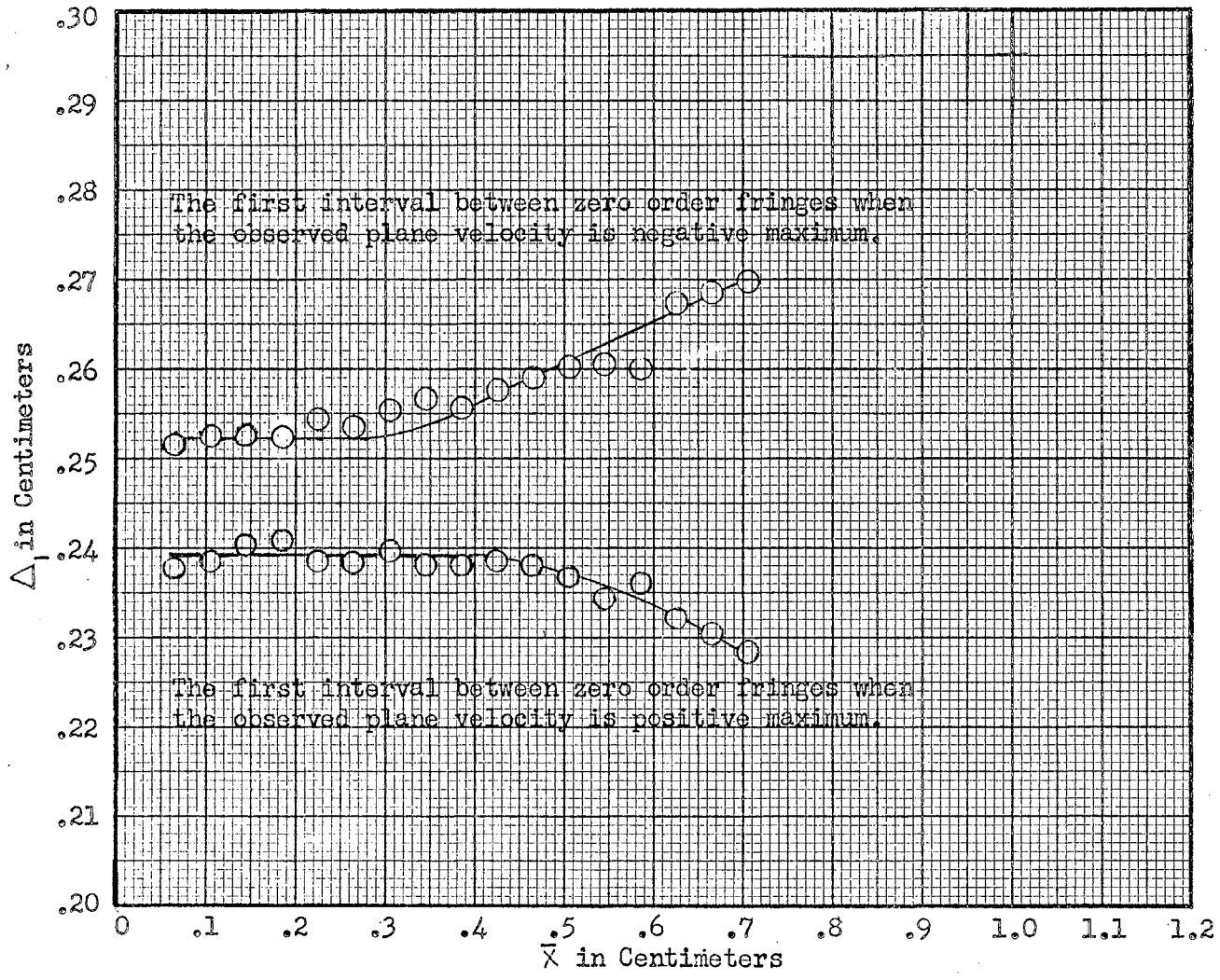

Figure 10. Δ_1 as a function of $\bar{X}$ for two successive Δ's for a 2.56 cm plane oscillating at 25 cps with a peak velocity amplitude of 4.362 cm/sec in a 1.30% milling yellow solution.

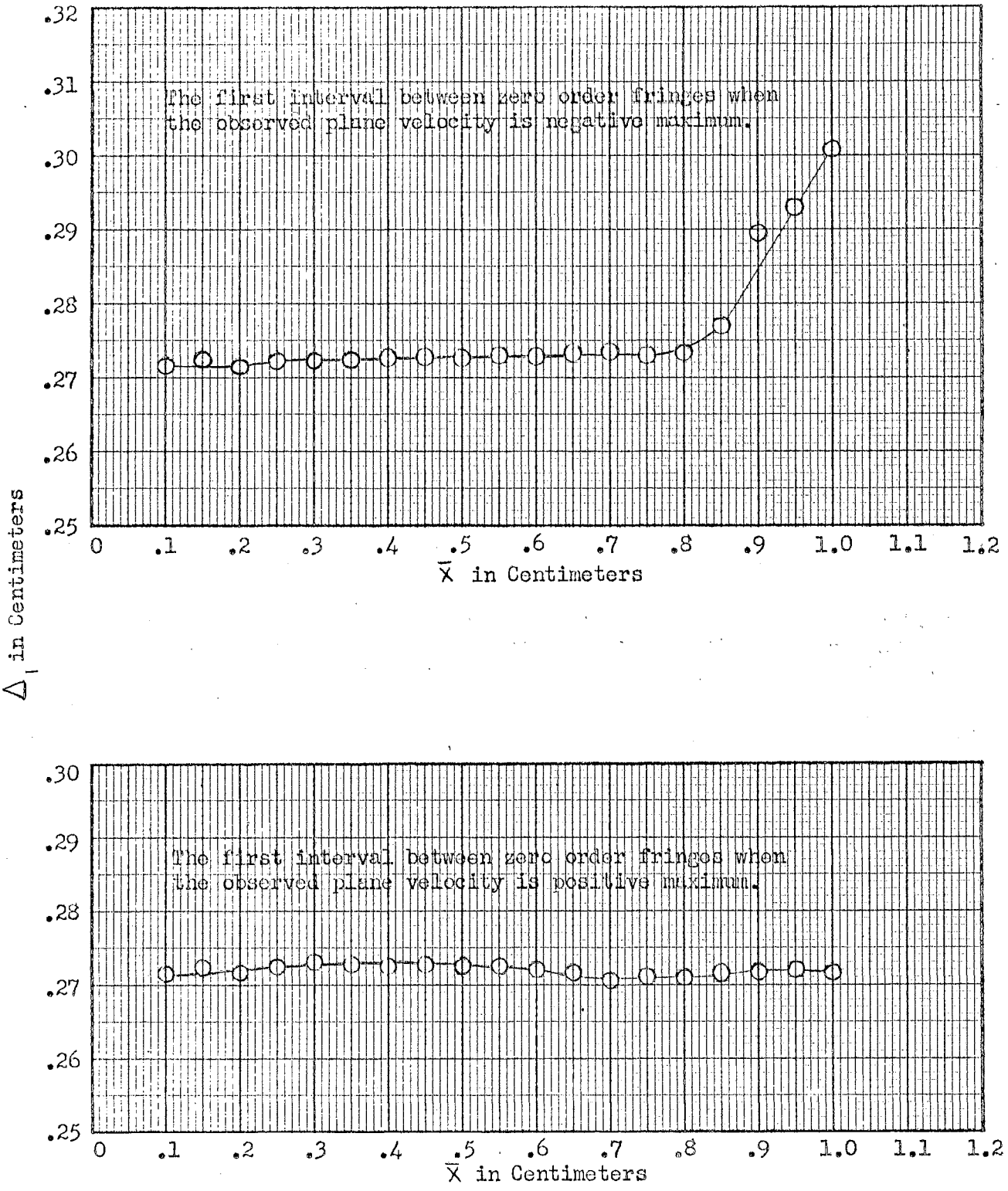

Figure 11. Δ_1 as a function of $\bar{X}$ for two successive Δ's for a 5.12 cm plane oscillating at 25 cps with a peak velocity amplitude of 2.181 cm/sec in a 1.30% milling yellow solution.

plane of infinite extent.

The effect of height of observation with respect to the bottom of the oscillating plane was determined from measurements of Δ_1 and Δ_2 as a function of height of observation. The results presented in figure 12 are for a 5.12 cm plane oscillating at 25 cps with a peak velocity amplitude of 2.181 cm/sec in a 1.30% milling yellow solution. The observed plane velocity is positive maximum. The deviations in Δ_1 and Δ_2 are approximately ±3%.

The spacing between the oscillating plane surface and the tank wall was varied and Δ_1 and Δ_2 measured. Results presented in figure 13 are for the same width, amplitude, concentration, and phase as for figure 12. The deviations in Δ_1 and Δ_2 are approximately ±3%.

In determining the possible effects of improper alignment of the polaroids for extinction, less than ±3% deviation was observed in the coordinates of zero order fringes when the polaroids were intentionally misaligned as much as 22.5°. Rotation of the entire polarizing system and measurement of zero order fringe coordinates showed similar deviations for rotations and misalignments of as much as 22.5°.

It was found that measurements of zero order fringe coordinates are reproducible to approximately ±.005 cm when the alignment of the microscope, plane, and tank is altered and realigned. Greater deviations are observed in $\overline{X}$ and lesser deviations are observed in the Δ's.

Tilting the oscillating plane so as not to oscillate in its own plane results in approximately ±3% deviation in the measured values of Δ_1. For moderate degrees of tilt, no definite trend is indicated in the deviations. The observed optical interference pattern appears to remain parallel to the oscillating plane.

For no change in the parameters of the flow and optical system, it

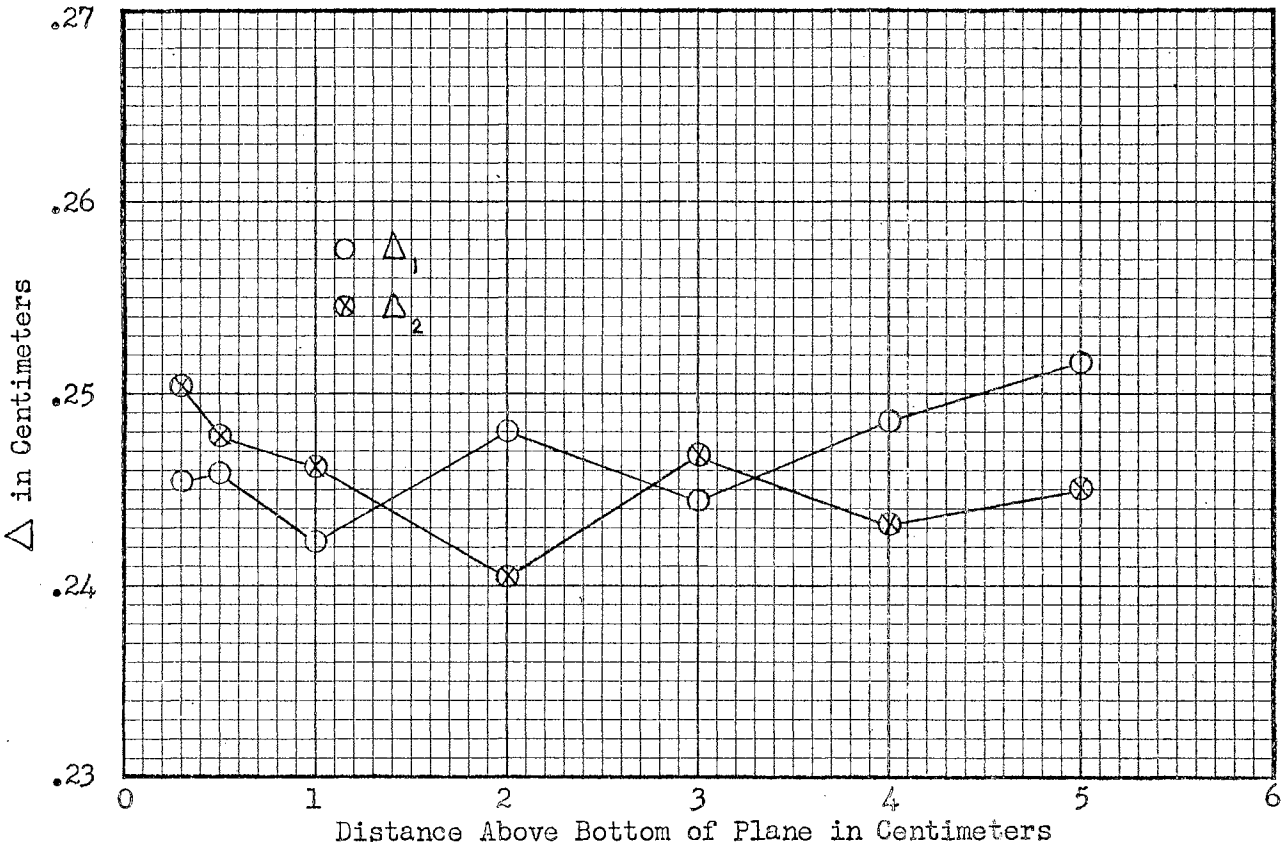

Figure 12. Δ_1 and Δ_2 as a function of height of observation from the bottom of the plane for a 5.12 cm plane oscillating at 25 cps with a peak velocity amplitude of 2.181 cm/sec in a 1.30% milling yellow solution. The observed plane velocity is positive maximum.

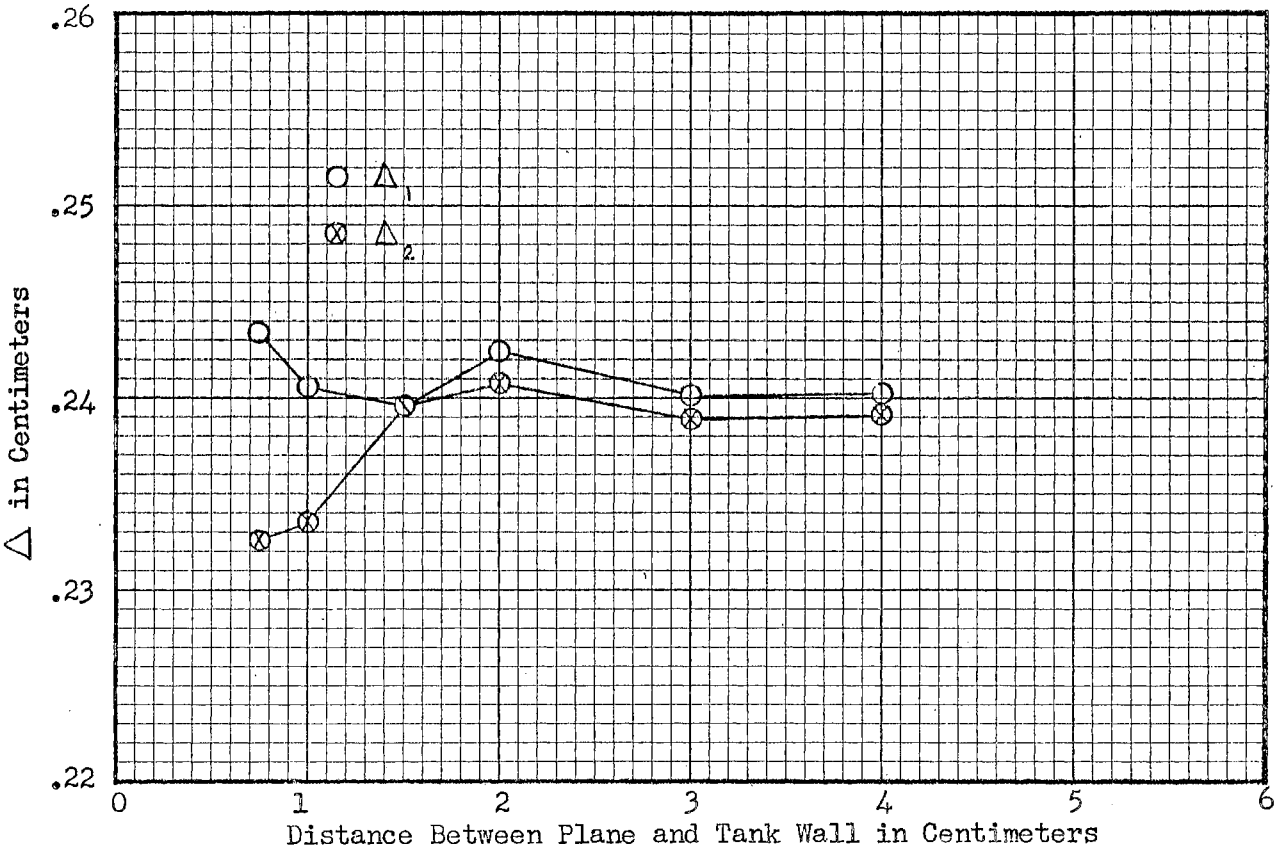

Figure 13. $\triangle_1$ and $\triangle_2$ as a function of spacing between the oscillating plane and the tank wall for a 5.12 cm plane oscillating at 25 cps with a peak velocity amplitude of 2.181 cm/sec in a 1.30% milling yellow solution. The observed plane velocity is positive maximum.

is found that a measurement of a coordinate of a fringe is reproducible to approximately ±.002 cm for a very well defined fringe. This represents ±1% of a typical value of Δ . For a less distinct fringe a coordinate measurement is reproducible to ±.005 cm or ±2% of Δ . Therefore, in a determination of Δ , the cumulative error due to errors at both ends of the interval could be ±3%. This error is comparable to the deviations in Δ 's observed in study of the effects of geometric parameters of the system. It is therefore concluded that the effects of reasonable variations in the geometric parameters result in variations, if any, which are less than the accuracy of measurement realized experimentally. It should be noted that temperature control was not provided in the experimental apparatus. Measurements were made at room temperature. Most measurements were made at 25°C, ±1°C. Data taken at different times may show slight lack of internal consistancy due to changes in the fluid properties with temperature.

CHAPTER IV

EXPERIMENTAL RESULTS

(a) Zero Order Fringe Propagation

The propagation of an observed zero order fringe was determined using techniques previously described. Results obtained for a 5.12 cm plane and for a 1.25 cm plane oscillating at 25 cps with peak velocity amplitudes of 1.507 cm/sec and 3.013 cm/sec respectively in a 1.30% milling yellow solution are presented in figure 14. Within the range of experimental errors, these data may be expressed in the form

$$\bar{x} = 14t \pm .28n \tag{4.1}$$

where $\bar{x}$ is the zero order fringe displacement in centimeters, t is time in seconds, and n is an integer or zero. $\bar{x} = 0$ is taken at the plane surface and $t = 0$ is chosen such that the plane velocity is zero when $t = 0$. The term $.28n$ appears to generalize the expression for any zero order fringe.

The experimentally determined zero order fringe propagation expressed in equation (4.1) indicates that the position of the zero order fringe approximately coincides with the point of zero velocity in the medium. That is, the fringe starts at the plane surface when the velocity of the plane is zero. This result differs from the theoretical equation for propagation as expressed by equation (2.39). Interpreting Δ to represent

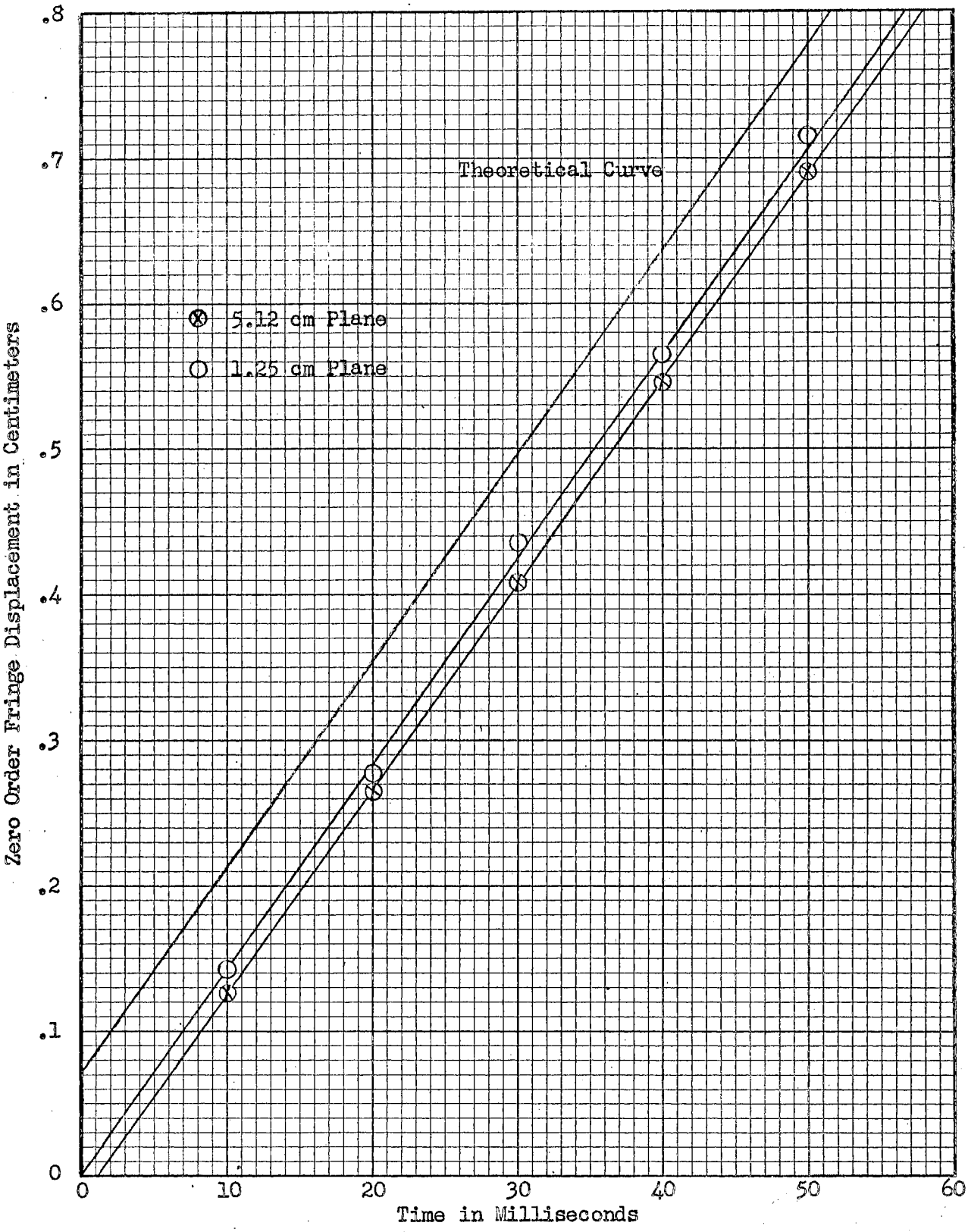

Figure 14. Zero order fringe displacement as a function of time for a 5.12 cm plane and for a 1.25 cm plane oscillating at 25 cps with peak velocity amplitudes of 1.507 cm/sec and 3.013 cm/sec respectively in a 1.30% milling yellow solution. Also shown is the theoretical propagation curve as given by equation (2.41), assuming the experimental slope.

$\lambda/2$, the points of zero shear in the shear wave would have to be shifted a distance of approximately $\lambda/8$ to coincide with the predicted zero order fringe location. This spacial shift corresponds to a phase shift of $\pi/4$ radians. Assuming the same velocity of propagation as experimentally determined, the theoretical propagation curve is also presented in figure 14. More precisely, the phase shifts for the two experimental curves of figure 14 are 41 degrees for the 1.25 cm plane and 54 degrees for the 5.12 cm plane.

(b) The Effect of Frequency of Oscillation

To study the effect of frequency of oscillation, Δ was determined as a function of frequency at a constant peak velocity amplitude and observed velocity phase of the oscillating plane. The frequency range obtainable at a given velocity amplitude was limited by the apparatus. Values of Δ were obtained for a 2.56 cm plane oscillating in a 1.30% milling yellow solution. The observed plane velocity was a positive maximum. Data obtained for a peak velocity amplitude of 0.436 cm/sec in the frequency range from 5 cps to 200 cps are presented in figure 15. The best straight line fit to these data, plotted on logarithmic coordinates, may be expressed by

$$\Delta = 3.9\, f^{-.85} \qquad (4.2)$$

where f is the frequency in cps. Results of similar measurements at a peak velocity amplitude of 1.745 cm/sec in the frequency range from 6.5 cps to 70 cps give the same expression as equation (4.2).

Further study of the effect of frequency of oscillation was made utilizing the higher order fringes observed in an interval Δ. For the observed plane velocity fixed at positive maximum, the peak plane velocity

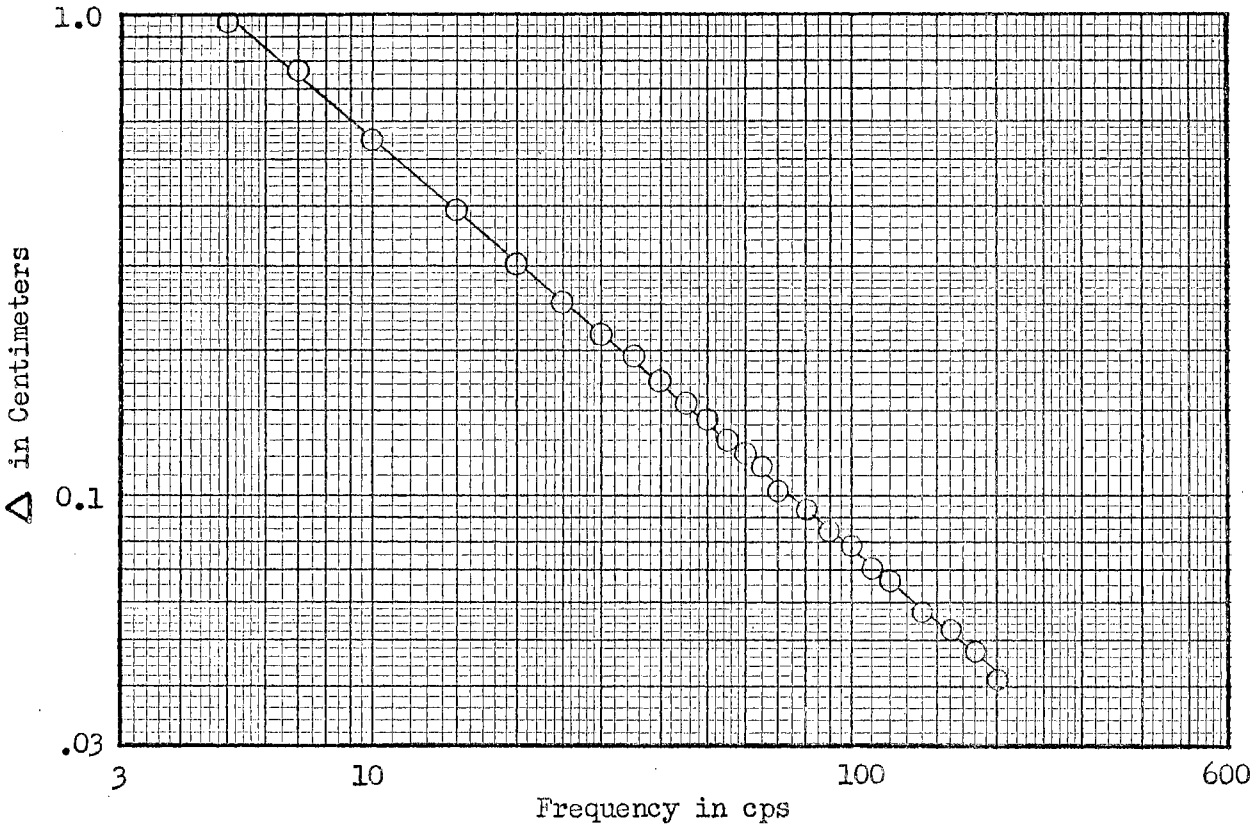

Figure 15. Δ as a function of frequency of oscillation for a 2.56 cm plane oscillating with a peak velocity amplitude of 0.436 cm/sec in a 1.30% milling yellow solution. The observed plane velocity is positive maximum.

at which the sharp transition from pattern (d) to pattern (e), as shown in figure 7, occurs was noted at various frequencies in the range from 5 cps to 50 cps. The occurrence of this transition indicates some characteristic magnitude of optical effect. Results obtained for a 2.56 cm plane oscillating in a 1.30% milling yellow solution are presented in figure 16. It is suggested that the increase in the transition peak plane velocity at frequencies below 15 cps may be due to wall interaction and/or the influence of finite extent of the plane. The increased viscous wavelength with decreased frequency supports this view.

(c) The Effect of Velocity Amplitude

Study of the effect of the peak velocity amplitude of the plane on the observed zero order fringes was made from various measurements of the interval Δ . No significant changes in Δ are observed to occur with variation in the peak velocity amplitude of the oscillating plane. Referring to results presented in figure 11, the zero order fringe spacing Δ is presented as a function of the distance $\bar{X}$ from the plane surface to the near side of the interval. These results show that Δ is constant for $\bar{X}$ ranging from essentially zero to approximately 3Δ . If Δ is interpreted as $\lambda/2$, and since equation (2.37) indicates a spacial attenuation rate of $\exp(-2\pi)$ per wavelength λ , then the velocity gradient varies by a factor of $\exp(-3\pi)$, which is approximately equal to 1.2×10^{4}. If the fluid can be characterized by a coefficient of viscosity, the constant value of Δ , interpreted as $\lambda/2$ indicates that under these experimental conditions, the coefficient of viscosity, related to λ by equation (2.32) is constant. This holds for a quite large variation of velocity gradient. For the data in figure 11, the peak magnitude of the velocity gradient at the plane surface is 35.6 sec^{-1}.

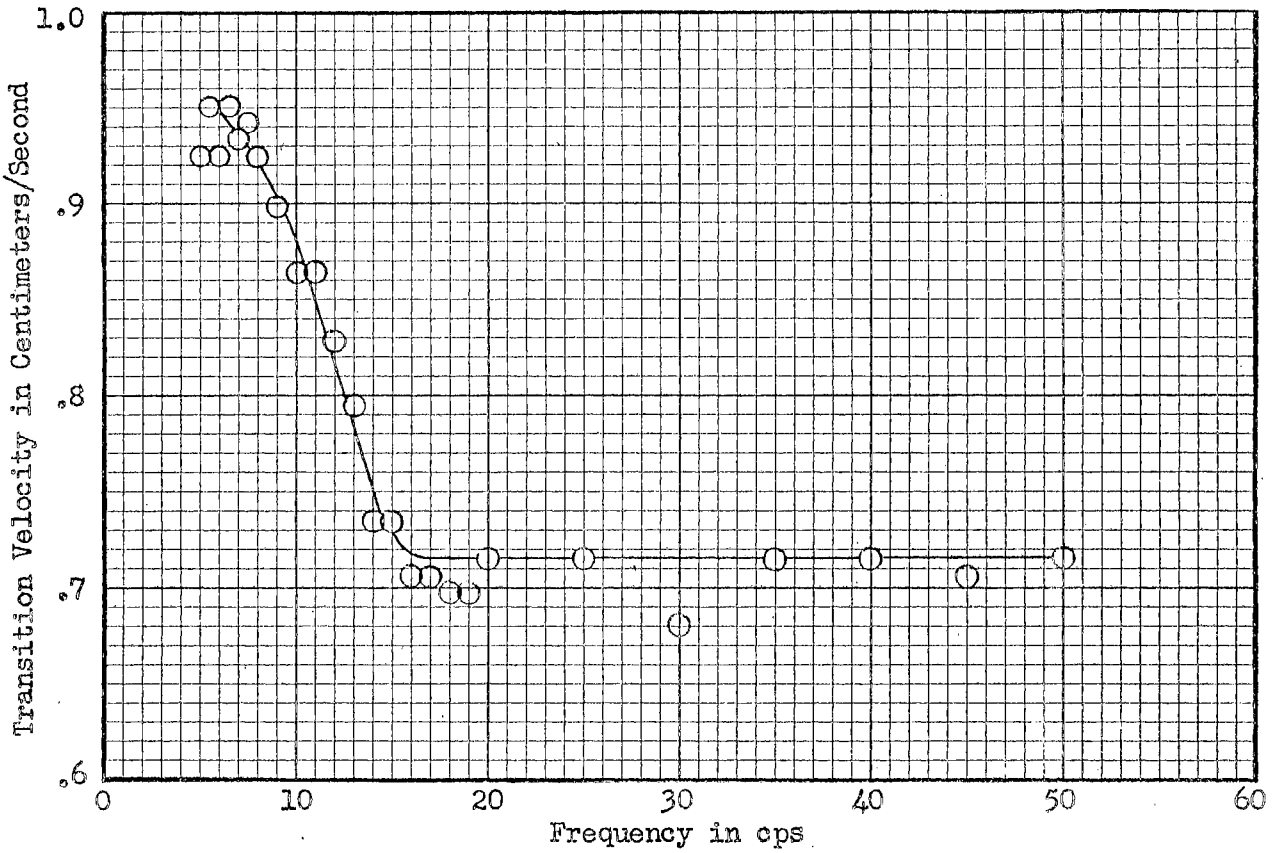

Figure 16. The plane velocity amplitude at which the transition from pattern (d) to (e) as shown in figure 7 occurs as a function of frequency of oscillation for a 2.56 cm plane in a 1.30% milling yellow solution. The observed plane velocity is positive maximum.

The range of velocity gradients for this case essentially covers the range of velocity gradients for which a 1.32% milling yellow solution is shown to be non-Newtonian in figure 17 of reference 12. The results are therefore not in agreement.

CHAPTER V

DISCUSSION OF RESULTS

It is found (see figure 14) that the velocity of propagation of a zero order fringe from an oscillating plane in aqueous milling yellow solution is constant when observed sufficiently close to the plane. This limit is determined by how nearly the plane of finite extent approximates a plane of infinite extent. As shown in Chapter IV, a phase discrepancy of approximately $\pi/4$ radians is found between theoretical and experimental results for zero order fringe propagation. It is possible that an optical end correction may be an important factor in accounting for the phase discrepancy. This optical end correction effect is due to the curved flow laminae around the edges of the oscillating plane. Some of the geometrical features applicable to edge effects are presented in Appendix B. Let the plane section of the oscillating plane approach zero, leaving only the edge condition. Measurements were made using an oscillating cylinder whose diameter is approximately equal to the thickness of the oscillating planes. Results of zero order fringe propagation measurements shown in figure 17 indicate that this limiting case of an oscillating cylinder differs from the experimentally determined propagation from an oscillating plane by a phase difference of approximately $\pi/4$ radians. Also shown in figure 17 is the fact that the observed zero order fringe propagation for an oscillating cylinder differs approximately $\pi/2$ radians in phase from the theoretical phase. This assumes that for the theoretical case a thin section normal to the optical path and passing through

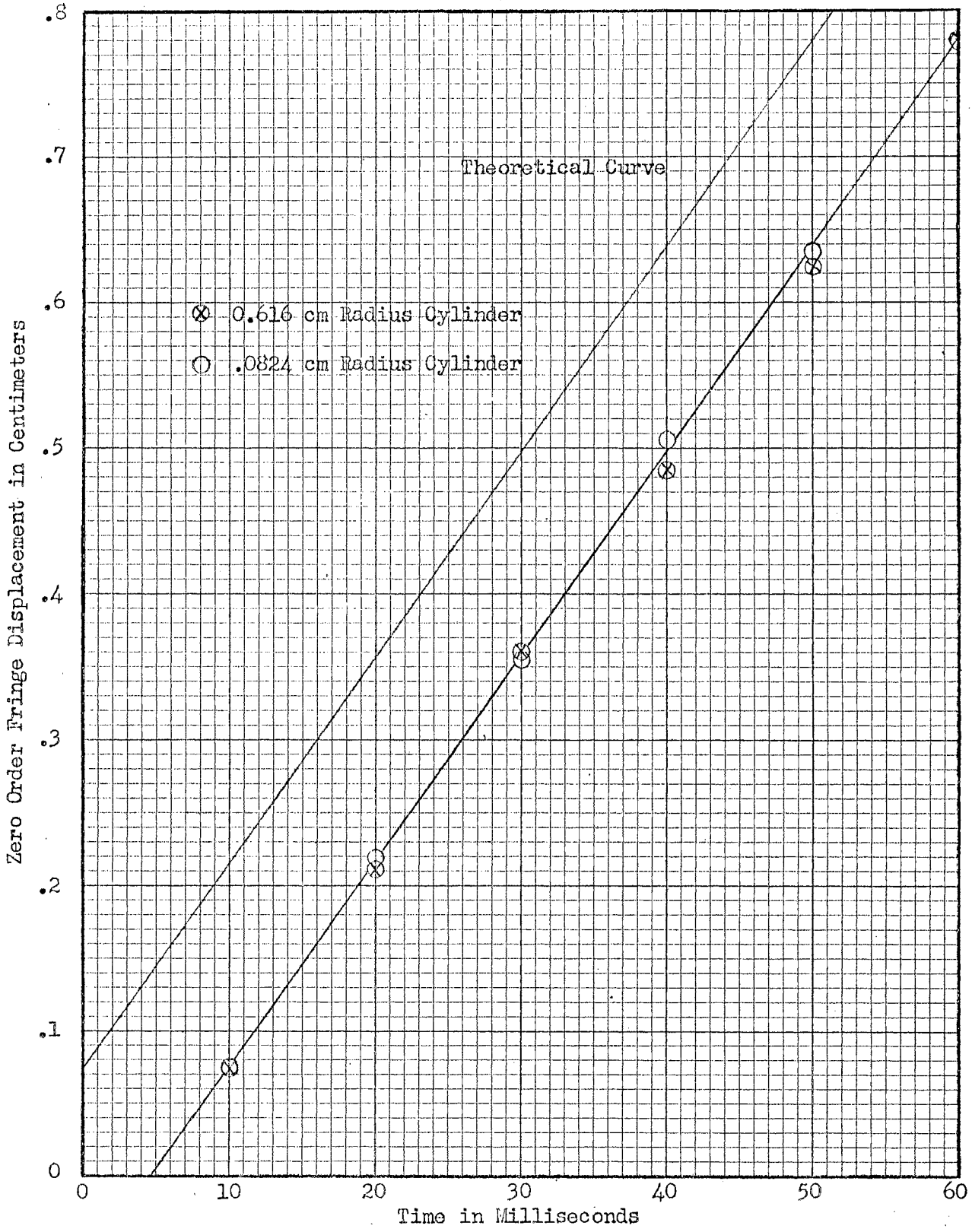

Figure 17. Experimental and theoretical zero order fringe displacements as functions of time for oscillating cylinders, oscillating at 25 cps in a 1.30% milling yellow solution.

the axis of the cylinder could be viewed. If the observed zero order fringe shift for an oscillating cylinder were used as an end correction and combined with the plane laminar section due to an oscillating plane, there would not necessarily result a full $\pi/2$ radian shift in observed zero order fringes. As these shifts are in the same direction, the phase difference between theoretical and experimental results for zero order fringe propagation from an oscillating plane is possibly due to an optical effect in the fringe areas at the plane edges. More detailed analysis of the oscillating cylinder is given in Appendix A.

Seeking further possible explanation for the phase discrepancy, consider the rheological properties of the medium. If the medium were behaving as an elastic solid, equation (2.36) becomes

$$\text{shearing stress} = G \frac{\partial \xi}{\partial X} \tag{5.1}$$

where G is a modulus of shear rigidity. With some elaboration on a treatment given by Eirich[18], the equation of motion for the purely elastic case and an oscillating plane becomes

$$\xi = -\frac{\dot{\xi}_o}{\omega} \cos\left[\omega t - \left(\frac{\rho}{G}\right)^{1/2} \omega X\right] \tag{5.2}$$

for the boundary condition that the plane velocity be given by

$$\dot{\xi} = \dot{\xi}_o \sin \omega t. \tag{5.3}$$

Then from equation (5.1) the shearing stress is zero for $\frac{\partial \xi}{\partial X} = 0$.

---

[18] Chapter II, reference 16.

From equation (5.2)

$$\frac{\partial \xi}{\partial x} = -\dot{\xi}_0 \left(\frac{\rho}{G}\right)^{1/2} \sin\left[\omega t - \left(\frac{\rho}{G}\right)^{1/2} \omega x\right]. \tag{5.4}$$

Following the same type of development as used in the derivation of equation (2.39) the propagation equation for a zero order fringe for the elastic case becomes

$$x = \left(\frac{G}{\rho}\right)^{1/2} \left[t \pm \frac{n\pi}{\omega}\right]. \tag{5.5}$$

This indicates that the position of a zero order fringe coincides with the point of zero velocity in the medium. The fact that this theoretical result gives agreement in phase with the experimentally determined zero order fringe propagation is not sufficient to establish that the medium is purely elastic. The experimental observations do indicate that the medium is behaving as if it were elastic. However, simply the fact that the medium is a fluid capable of unrecoverable viscous flow indicates that it is not purely elastic. The rheological characterization appropriate to the fluid may be that of a viscoelastic medium, where the elastic behavior is dominant for the experimental conditions here employed.

Another possible source of the phase discrepancy between theoretical and experimental results for zero order fringe propagation may be the flow-optic relation. The possibility that the stress dependence is totally erroneous is mentioned but will not be further considered. However, it should be noted that for a viscoelastic medium, the stress-strain relation involves both the displacement gradient and the velocity gradient.

Consider the experimentally determined frequency dependence of as expressed in equation (4.2). This states that Δ is proportional to

the (-.85) power of the frequency. From theoretical equation (2.32), interpreting Δ to represent $\lambda/2$, the frequency dependence of Δ should be on the (-.50) power of the frequency. For an elastic medium, the wavelength of a transverse wave is inversely proportional to the first power of the frequency. The fact that the experimentally determined frequency dependence of Δ falls between the theoretical frequency dependence for the viscous and for the elastic case is an indication of viscoelastic behavior. Here, as in the consideration of the phase discrepancy, the results indicate a dominance of elastic behavior. This dominance follows from the fact that (-.85) power is nearer to (-1.0) power than to (-.50) power dependence.

Interpreting Δ to represent $\lambda/2$ and neglecting the phase discrepancy, an apparent coefficient of viscosity may be derived. From the data presented in figure 14 and as expressed by equation (4.1), the velocity of propagation V is 14 cm/sec. Using equation (2.33) which expresses V in terms of viscosity, density, and angular frequency, the expression for the coefficient of kinematic viscosity $\nu = \mu/\rho$ is

$$\nu = \frac{V^2}{2\omega} \tag{5.6}$$

where ν is in stokes when the cgs system of units are used. Denoting an experimental value by $\bar{\nu}$, the experimental conditions of figure 14 give $\bar{\nu}$ = 62.4 centistokes. This value is in the range of values reported elsewhere.[13] Δ, and therefore the velocity of propagation, has been found quite insensitive to variations in the velocity gradient by a factor of 1.2×10^4. This indicates a constant apparent coefficient of kinematic viscosity over a wide range of velocity gradients. The velocity gradients are within the range of gradients for which the viscosity is reported non-Newtonian in figure 17 of reference 12.

It is proposed that the application of the oscillating plane to the determination of the amount of birefringence (difference between indices of refraction) be investigated. The basis for measurement of this amount of birefringence is the equation for relative retardation as pertains to appearance of higher order fringes as is given by equation (2.16). Working with monochromatic light, stroboscopic illumination, and starting with sufficiently low amplitude that the entire field of view is dark, the amplitude of oscillation of the plane is increased. Light areas will then appear thus revealing the location of zero order fringes. When the amplitude of vibration is sufficient a dark fringe will appear in the bright area nearest the plane. This is then a first order fringe for which the relative retardation is one wavelength in air. Knowing the wavelength of the light and the effective length of the optical path (which due to edge effects may differ significantly from the plane width), the differences of the indices of refraction may be computed. Corresponding to the appearance of this first order fringe, the velocity of the oscillating plane may be determined and based on the work described herein, the velocity gradient at the location of the fringe may be determined. The amplitude of oscillation may then be increased. The first order fringe will then divide and at a sufficiently increased amplitude a second order fringe will appear. Again the amount of birefringence and velocity gradient may be determined. This may be continued for still higher order fringes. By varying the plane width the part played by the edge effects might be eliminated. Also by varying plane width intermediate values of amount of birefringence for intermediate velocity gradients may be determined. An optical compensator may also be used to determine intermediate values. Thus the effect of velocity gradient on the difference of indices of refraction may be studied. This method would have the distinct advantage over the conventional method of the rotating concentric cylinder

apparatus in that frequency dependence of the amount of birefringence may also be studied. It should be noted that should edge effects not interfere, the location of these higher order fringes with respect to the zero order fringes may be used as a check of the spacial decrease of velocity gradient as the higher order fringes will first appear at the point of maximum velocity gradient between the zero order fringes.

Consider the instantaneous state of stress of the medium along a line perpendicular to an infinite oscillating plane. Shearing stress at all points along this line will be directed parallel to the plane but with varying magnitude and direction. Similarly the orientation of the principal stresses will be the same at all points but with varying magnitude and direction. If the extinction angle (see Appendix B) were independent of the magnitude of the principal stresses and dependent only on their orientation, then by viewing the region with crossed polarizers and rotating the plane of the polarizers with respect to that of the oscillating plane, the entire field would darken when the angle between the two planes was the extinction angle. However, as in general the extinction angle is dependent on the magnitude of the principal stresses the darkening would occur in bands parallel to the oscillating plane and at positions dependent on the relation between the extinction angle and the velocity gradient. Should these bands (isoclines) be sufficiently well defined this might be used as a basis for study of stress and frequency dependence of extinction angle for the medium.

It is suggested that further work be carried out to investigate the possibility of viscoelastic properties of aqueous milling yellow solutions. A dynamic technique, as here employed, with provisions for working at larger velocity amplitudes and over a wider range of frequencies, may reveal significant indications of non-Newtonian viscosity and viscoelastic behavior. Results could be presented in terms of an impedance to shear.

Temperature and concentration effects should be investigated under dynamic conditions. Study of the basic structure of milling yellow solutions and the physical mechanism of the optical birefringence should be undertaken. In view of the importance of edge effects, further study directed specifically toward determination of these edge effects would be of considerable value.

BIBLIOGRAPHY

Alcock, E. D., and C. D. Sadron, "An Optical Method for Measuring the Distribution of Velocity Gradients in a Two-Dimensional Flow". Physics, 6, 92-95 (1935).

Balint, E., "Techniques of Flow Visualization", Aircraft Engineering, 25, 161-167 (1953).

Coker, E. G., and L. N. G. Filon, A Treatise on Photo-Elasticity (Cambridge University Press, London, 1931).

Dewey, D. R., "Visual Studies of Fluid Flow Patterns Resulting From Streaming Double Refraction", Unpublished Doctoral Dissertation, Massachusetts Institute of Technology, 1941.

Edsall, J. T., "Streaming Birefringence and Its Relation to Particle Size and Shape", Advances in Colloid Science (Interscience Publishers, Inc., New York, 1942), Vol. I.

Edsall, J. T., A. Rich, and M. Goldstein, "Instrument for the Study of Double Refraction of Flow at Low and Intermediate Velocity Gradients", Rev. Sci. Inst., 23, 695 (1952).

Eirich, F. R., Rheology (Academic Press Inc., New York, 1956), Vol. I.

Ferry, J. D., "Studies of Mechanical Properties of Substances of High Molecular Weight, I. A Photoelastic Method for Study of Transverse Vibrations in Gels", Rev. Sci. Inst., 12, 79-82 (1941).

Frank, N. H., Introduction to Electricity and Optics, Second Edition (McGraw-Hill Book Company, Inc., New York, 1952).

Frocht, M. M., Photoelasticity (John Wiley and Sons, Inc., New York, 1948), Vol. II.

Hargrove, L. E., Jr., and G. B. Thurston, "Photographic Method for Analysis of Fluid Motion", J. Acoust. Soc. Am., 29, 179 (A) (1957).

Hauser, E. A., and D. R. Dewey, "Study of Liquid Flow", Ind. Eng. Chem., 31, 786 (1939).

Honeycutt, E. H., Jr., and F. N. Peebles, "A Study of Laminar Flow Phenomena Utilizing a Doubly Refracting Liquid", Progress Report 3 "Rheological Properties of Aqueous Solutions of Milling Yellow Dye", Published Master's Thesis under Contract No. Nonr-811(04), Knoxville, Tennessee, Engineering Experiment Station and Department of Chemical Engineering of the University of Tennessee (1955).

Humphry, R. H., "Demonstrations of Double Refraction Due to Motion of a Vanadium Pentoxide Sol and Some Applications", Proc. Roy. Soc. (London), 35, 217-218 (1923).

Jessop, H. T., and F. C. Harris, Photoelasticity: Principles and Methods (Dover Publications, Inc., New York, 1950).

Lamb, H., Hydrodynamics (Dover Publications, Inc., New York, 1932).

Maxwell, J. C., "On Double Refraction in a Viscous Fluid in Motion", Proc. Roy. Soc., 22, 46-47 (1873).

McLachlan, N. W., Bessel Functions for Engineers (Oxford at the Clarendon Press, London, 1955).

Peebles, F. N., H. J. Garber, and S. H. Jury, "Preliminary Studies of Flow Phenomena Utilizing a Doubly Refracting Liquid", Proc. Third Midwestern Conference on Fluid Mechanics, Minneapolis: The University of Minnesota Press, 1953.

Peebles, F. N., J. W. Prados, and E. H. Honeycutt, Jr., "A Study of Laminar Flow Phenomena Utilizing a Doubly Refracting Liquid", Progress Report 1 under Contract No. Nonr-811(04), Knoxville, Tennessee, Engineering Experiment Station and Department of Chemical Engineering of the University of Tennessee (1955).

Prados, J. W., and F. N. Peebles, "A Study of Laminar Flow Phenomena Utilizing a Doubly Refracting Liquid", Progress Report 2 "Determination of the Flow Double Refraction Properties of Aqueous Milling Yellow Dye Solutions", Published Master's Thesis under Contract No. Nonr-811(04), Knoxville, Tennessee, Engineering Experiment Station and Department of Chemical Engineering of the University of Tennessee (1955).

Rosenberg, B., "The Use of Doubly Refracting Solutions in the Investigation of Fluid Flow Phenomena", Navy Dept. David W. Taylor Model Basin, Washington 7, D. C., Report No. 617, 1952.

Sears, F. W., Principals of Physics - Optics (Addison-Wesley Press, Inc., Cambridge, 1948).

Weller, R., "The Optical Investigation of Fluid Flow", J. App. Mech., 14, 103-107 (1947).

Weller, R., D. J. Middlehurst, and R. Steiner, "The Photoviscous Properties of Fluids", NACA Tech. Note No. 841 (1942).

APPENDIX A

THEORETICAL AND EXPERIMENTAL CONSIDERATION OF AN OSCILLATING CYLINDER

(a) Theory

Consider the problem of an oscillating cylinder with its axis coincident with the Y axis. The cylinder, infinite in extent in the Y direction and of radius r_o, is immersed in an infinite expanse of viscous fluid and is caused to oscillate along its axis. Let the motion of the cylinder be given by

$$\dot{\xi} = \dot{\xi}_o \exp[i\omega t] \tag{A.1}$$

where

$\dot{\xi}$ = first time derivative of displacement in the Y direction

$\dot{\xi}_o$ = peak velocity amplitude of the cylinder.

Consider the forces acting on a cylindrical volume element of fluid. The inertial force is

$$f_i = ma = 2\pi r \ell \rho dr \ddot{\xi} \tag{A.2}$$

where

m = mass

a = acceleration

ℓ = length of the element in the Y direction

ρ = fluid density

dr = thickness of the volume element in the r direction

$\ddot{\xi}$ = second time derivative of displacement in the Y direction.

The shear force acting on the volume element is

$$f_s = \frac{\partial}{\partial r}\left[2\pi r \ell \mu \frac{\partial \dot{\xi}}{\partial r}\right] dr \tag{A.3}$$

where μ is the fluid viscosity. Equating the forces given in equations (A.2) and (A.3) and simplifying results gives the partial differential equation

$$(\mu/\rho)\left[r\frac{\partial^2 \dot{\xi}}{\partial r^2} + \frac{\partial \dot{\xi}}{\partial r}\right] = r\frac{\partial \dot{\xi}}{\partial t} \tag{A.4}$$

where the fluid viscosity has been considered constant. Assume a solution of the form

$$\dot{\xi} = R(r)\,T(t) \tag{A.5}$$

where $R(r)$ and $T(t)$ represent functions of r alone and t alone, respectively. Substitution of $\dot{\xi}$ from equation (A.5) into equation (A.4) permits separation of the variables. Setting the separated members equal to a constant K gives the two ordinary differential equations

$$\frac{d^2R(r)}{dr^2} + \frac{1}{r}\frac{dR(r)}{dr} - \frac{K\rho}{\mu}R(r) = 0 \tag{A.6}$$

and

$$\frac{dT(t)}{dt} - KT(t) = 0. \tag{A.7}$$

A solution to equation (A.7) is

$$T(t) = \exp\left[Kt\right]. \tag{A.8}$$

From equations (A.1) and (A.8) it follows that

$$K = i\omega \tag{A.9}$$

and

$$T(t) = \exp\left[i\omega t\right]. \tag{A.10}$$

Combining equations (A.6) and (A.9)

$$\frac{d^2R(r)}{dr^2} + \frac{1}{r}\frac{dR(r)}{dr} - i\frac{\omega\rho}{\mu}R(r) = 0. \tag{A.11}$$

Equation (A.11) is Bessel's differential equation. A solution[19] to equation (A.11) is

$$R(r) = A J_0\left[\left(\frac{\omega\rho}{\mu}\right)^{1/2} r i^{3/2}\right] + B K_0\left[\left(\frac{\omega\rho}{\mu}\right)^{1/2} r i^{1/2}\right] \tag{A.12}$$

where

$J_n(\zeta)$= functional notation for a Bessel function of the first kind of order n and argument ζ.

$K_n(\zeta)$= functional notation for a modified Bessel function of the second kind of order n and argument ζ.

Since

$$J_0\left[\left(\frac{\omega\rho}{\mu}\right)^{1/2} r i^{3/2}\right] \longrightarrow \infty \quad \text{as} \quad r \longrightarrow \infty \tag{A.13}$$

---

[19] N. W. McLachlan, Bessel Functions for Engineers (Oxford at the Clarendon Press, London, 1955).

then the constant A must be zero. The solution becomes

$$\dot{\xi} = B \exp[i\omega t] K_0\left[\left(\frac{\omega\rho}{\mu}\right)^{1/2} r\, i^{1/2}\right]. \tag{A.14}$$

When $r = r_0$, equation (A.1) requires that

$$B = \frac{\dot{\xi}_0}{K_0\left[\left(\frac{\omega\rho}{\mu}\right)^{1/2} r_0\, i^{1/2}\right]} \tag{A.15}$$

and the solution to equation (A.4) becomes

$$\dot{\xi} = \dot{\xi}_0 \exp[i\omega t] \frac{K_0\left[\left(\frac{\omega\rho}{\mu}\right)^{1/2} r\, i^{1/2}\right]}{K_0\left[\left(\frac{\omega\rho}{\mu}\right)^{1/2} r_0\, i^{1/2}\right]}. \tag{A.16}$$

Using the relation

$$i^{-n} K_n(\zeta i^{1/2}) = \mathrm{ker}_n \zeta + i\, \mathrm{kei}_n \zeta = N_n(\zeta) \exp[i\phi_n(\zeta)]$$

equation (A.16) may be written in the form

$$\dot{\xi} = \dot{\xi}_0 \frac{N_0\left[\left(\frac{\omega\rho}{\mu}\right)^{1/2} r\right]}{N_0\left[\left(\frac{\omega\rho}{\mu}\right)^{1/2} r_0\right]} \exp\left[\left[i\left\{\omega t + \phi_0\left[\left(\frac{\omega\rho}{\mu}\right)^{1/2} r\right] - \phi_0\left[\left(\frac{\omega\rho}{\mu}\right)^{1/2} r_0\right]\right\}\right]\right]. \tag{A.17}$$

Let the equation of motion of the oscillating cylinder be defined by

$$\dot{\xi} = \dot{\xi}_0 \,\mathrm{SIN}\, \omega t. \tag{A.18}$$

The corresponding form of the equation of motion for the fluid becomes, from equations (A.17) and (A.18),

$$\dot{\xi} = \dot{\xi}_0 \frac{N_0\left[\left(\frac{\omega\rho}{\mu}\right)^{1/2} r\right]}{N_0\left[\left(\frac{\omega\rho}{\mu}\right)^{1/2} r_0\right]} \operatorname{SIN}\left\{\omega t + \Phi_0\left[\left(\frac{\omega\rho}{\mu}\right)^{1/2} r\right] - \Phi_0\left[\left(\frac{\omega\rho}{\mu}\right)^{1/2} r_0\right]\right\}. \quad (A.19)$$

Also, for the equation of motion as specified by equations (A.18) and (A.19), the gradient of the velocity is

$$\frac{\partial \dot{\xi}}{\partial r} = \dot{\xi}_0 \left(\frac{\omega\rho}{\mu}\right)^{1/2} \frac{N_1\left[\left(\frac{\omega\rho}{\mu}\right)^{1/2} r\right]}{N_0\left[\left(\frac{\omega\rho}{\mu}\right)^{1/2} r_0\right]} \operatorname{SIN}\left\{\omega t + \Phi_1\left[\left(\frac{\omega\rho}{\mu}\right)^{1/2} r\right] - \Phi_0\left[\left(\frac{\omega\rho}{\mu}\right)^{1/2} r_0\right] - \frac{\pi}{4}\right\}. \quad (A.20)$$

Values of N_0, N_1, Φ_0, and Φ_1 are tabulated in McLachlan[19] and in other tables of Bessel functions. By letting $\frac{\partial \dot{\xi}}{\partial r} = 0$ in equation (A.20), the equation for propagation of a point where the gradient of the velocity is zero is found to be

$$\omega t = \pm n\pi + \frac{\pi}{4} + \Phi_0\left[\left(\frac{\omega\rho}{\mu}\right)^{1/2} r_0\right] - \Phi_1\left[\left(\frac{\omega\rho}{\mu}\right)^{1/2} r\right]. \quad (A.21)$$

For $\left[(\omega\rho/\mu)^{1/2} r_0\right] > 10$, equation (A.21) may be approximated by

$$\omega t \simeq \left[(\omega\rho)/(2\mu)\right]^{1/2} (r - r_0) + \frac{3\pi}{4} \pm n\pi \quad (A.22)$$

with errors $\leq 2°$. Solving equation (A.22) for $(r - r_0)$ gives the distance from the cylinder boundary to a point where the gradient of the velocity is zero as a function of time. The expression is

$$(r - r_o) \simeq \left[(2\mu)/(\omega\rho)\right]^{1/2}\left(\omega t + \frac{\pi}{4} \pm n\pi\right). \qquad (A.23)$$

$(r - r_o)$ as given by equation (A.23) is identical in form with equation (2.39). This is to be expected since in the derivation of equation (A.23) an approximation is made which is permissible only for $\left[(\omega\rho/\mu)^{1/2} r_o\right] > 10$. This condition validating the approximation infers that the ratio of the radius of curvature of the cylinder to the viscous wavelength must be large. Obviously, for r_o much greater than the viscous wavelength, the case of the oscillating plane is approached.

A distinguishing factor between the oscillating cylinder and the oscillating plane of finite dimensions is that for the cylinder the fluid motion along an optical path can be analytically expressed. For the oscillating plane, an unknown edge condition exists.

(b) Experiment

The propagation of observed zero order fringes due to oscillating cylinders was determined. Results obtained for a 0.616 cm radius cylinder and for a .0824 cm radius cylinder oscillating at 25 cps with a peak velocity amplitude of 5.081 cm/sec in a 1.30% milling yellow solution are presented in figure 17. Within the range of experimental errors, these data may be expressed in the form

$$(r - r_o) = 14\,(t - .005) \pm .28n \qquad (A.24)$$

where $(r - r_o)$ is the zero order fringe displacement in centimeters, t is time in seconds, and n is an integer or zero. $t = 0$ is chosen such that the plane velocity is zero when $t = 0$. The term $.28n$ appears to

generalize the expression for any zero order fringe.

Assuming that a thin section normal to the optical path and passing through the axis of the cylinder could be viewed, equation (A.23) would be the theoretical equation for propagation of a zero order fringe. However, the result expressed by equation (A.24) is integrated optical effect along the entire path. Assuming the experimental slope, equation (A.23) is represented in figure 17. From the collected results shown in figure 17, it is likely that the result of the integrated optical effect along the optical path is to cause the observed zero order fringe propagation to differ from equation (A.23) by a phase of approximately 85 degrees. However, this conclusion is subject to the same uncertainties as pertain to the properties of the fluid as are discussed in Chapter V.

APPENDIX B

STRESS-OPTIC AND FLOW-OPTIC RELATIONS

(a) Methods of Description of Optical Effects

A uniaxial crystal has only one optic axis. In the ray treatment of double refraction this optic axis is defined[20] as a direction of light propagation for which the velocity of propagation is independent of the plane of polarization of the light. This propagation velocity is called the ordinary velocity. Expressed in terms of the direction of the electric vector, if the x axis of an x-y-z-rectangular coordinate system is taken as the optic axis, then the velocity of propagation along the x axis is independent of the orientation of the electric vector in the y-z plane. Should the electric vector point in the y direction light will propagate in the z direction with the ordinary velocity. However, for propagation in the z direction with the electric vector in the x direction, the velocity of propagation will have an extreme difference from the ordinary velocity. This velocity is then called the extraordinary velocity. The crystal is then termed positive or negative uniaxial in accordance as the ordinary velocity is respectively greater than or less than the extraordinary velocity. Should the electric vector have both x and y components, the two components will propagate in the z direction with

---

[20] N. H. Frank, Introduction to Electricity and Optics, Second Edition (McGraw-Hill Book Company, Inc., New York, 1950), p. 345.

different velocities, thus undergoing relative phase shift. This will generally give rise to elliptically polarized light.

Description of double refraction according to Huygen's wavelets[21] in the case of a uniaxial crystal is accomplished by assuming that each point on a wave front gives rise to two wavelet surfaces. One of these surfaces is spherical as is normally assumed for isotropic media. The second surface is ellipsoidal. The ellipsoid is in contact with the sphere at two points on a diagonal of the sphere. The direction defined by this diagonal is that of the optic axis of the crystal. This is equivalent to defining the optic axis as that direction of propagation for which the wave fronts constructed from the two wavelet surfaces propagate with the same velocity. Propagation in other directions gives rise to two wave fronts propagating with different velocities. In some cases the ray directions derived from these wave fronts are also different. This simplified wavelet treatment of double refraction is useful in describing the displacement of ordinary and extraordinary rays sometimes obtained on passage through crystal elements. However, lack of reference to plane of polarization in definition of optic axis limits the general utility of this method of description.

The properties of the medium determining the propagation of light can be measured along three mutually perpendicular directions, called principal axes.[22] Call these axes x, y, and z. Locate a point x' on the x axis such that x' equals the reciprocal of the velocity of propagation in the y-z plane and for the electric vector having only x component.

---

[21] F. W. Sears, Principles of Physics - Optics (Addison-Wesley Press, Inc., Cambridge, 1948), p. 176.

[22] H. T. Jessop and F. C. Harris, Photoelasticity: Principals and Methods (Dover Publications, Inc., New York, 1950), p. 56.

Similarly locate y' and z' corresponding to electric vectors oriented in the y and z directions. Form an ellipsoid x' , y', and z' located on its surface. This ellipsoid so formed is called Fresnel's ellipsoid of elasticity. For an electric vector of arbitrary direction the distance from the origin to the point on the ellipsoid defined by that direction gives the reciprocal of the velocity of propagation of the ray. Consider the case where y' and z' are equal. Then the x direction is that of an optic axis. Let a ray pass through the origin and locate its wave front in coincidence with the origin. The point at which the wave front cuts the circle of radius y' (z') in the y-z plane may be used to define an axis which passes through the origin and this point of intersection. A second axis is selected perpendicular to the first. These two axes are called principal axes in the plane of the wave front. Light will be resolved into two components along these two axes. The component resolved along the first axis will propagate with the ordinary velocity and the other component with some other velocity. In the case x', y', and z' are all equal the medium is isotropic. In the case no two of these are equal the system acts as a biaxial crystal.

(b) Stress-optic Relations of Maxwell and Neumann for Solids

The stress-optic relations as developed by Maxwell and Neumann for solids are clearly enunciated by Frocht[23] as follows:

> We define secondary principal stresses for a given direction (ζ) as the principal stresses resulting from the stress components which lie in a plane normal to the given direction (ζ) , and denote these by $(P', Q')_{\zeta}$.
>
> At each point of a stressed body there exists only one set of primary principal stresses. However, there exists at the same point

---

[23] M. M. Frocht, Photoelasticity (John Wiley and Sons, Inc., New York, 1948), Vol. II, pp. 333-335.

an infinite number of secondary principal stresses, depending on the choice of direction through the given point.

When a polarized beam enters a stressed medium it is resolved into components which are parallel to the secondary principal stresses corresponding to the given ray at the point of entrance.

The vibrations associated with the beam of light passing through the stressed body are at each point parallel to the directions of the secondary principal stresses, for the given ray.

When the secondary principal stresses remain constant between the point of entrance and the point of exit, the retardation in wavelengths or fringes is given by

$$n = C(P' - Q')T \tag{B.1}$$

in which C is the usual stress-optic coefficient, T is the actual light path, and P' and Q' are the secondary principal stresses for the direction of the given ray.

If only the directions of the secondary principal stresses remain constant and the magnitudes vary, then

$$n = C\int (P' - Q')\, dT. \tag{B.2}$$

(c) Stress-optic Relations for Fluids

The statement that the vibrations associated with the beam of light passing through a stressed solid are at each point parallel to the directions of the secondary principal stresses does not necessarily apply to fluids. In a viscous fluid in laminar motion the primary principal stresses at a point consist of a tension and a compression oriented at 45° to the flow line at the point.[24] To investigate the orientation of the vibrations of a beam of light with respect to the stresses, a concen-

[24] E. G. Coker and L. N. G. Filon, A Treatise on Photo-Elasticity (Cambridge University Press, London, 1931), p. 284.

tric cylinder apparatus[25] is used. The fluid is contained in the annular gap between concentric cylinders, one fixed and the other rotating with a uniform angular velocity. The apparatus is placed between crossed polarizers. It follows from extension of the behavior of solids to fluids that if the directions of polarization in the fluid are along the directions of principal stresses, dark lines should appear along radii which are oriented at 45° with respect to the axes of the polarizers. However, it is found that the dark lines make an angle χ, called the extinction angle, with the axes of the polarizers. Observed values of the extinction angle range between the limits of 0° and 45° and are also found to be a function of the velocity gradient.[26] The extinction angle is defined by Edsall[27] as the angle made by the optic axis of the flow-birefringent fluid with the streamline. The measurement of extinction angle with the concentric apparatus does not specifically test for the existance of optic axes as defined in section (a) of this appendix.

(d) Mechanisms for the Optical Effects[16]

Birefringence has been observed in suspensions of geometrically and optically anisotropic molecules or particles. In laminar flow, the Brownian motion tends to counteract the hydrodynamic orientation. Both influences establish the actual angular distribution of the particles and yield the extinction angle as the direction of maximum or minimum angular density. The birefringence follows as the difference of the corresponding

---

[25] J. T. Edsall, A. Rich, and M. Goldstein, Rev. Sci. Inst., 23, 695 (1952).

[26] p. 616, reference 16.

[27] J. T. Edsall, "Streaming Birefringence and Its Relation to Particle Size and Shape", Advances in Colloid Science (Interscience Publishers, Inc., New York, 1942), Vol. I, pp. 296-316.

densities multiplied by the optical anisotropy of the single particle. In general, the direction of the maximum and minimum angular densities are not simply related to the streamlines, but differ by the extinction angle. The extinction angle becomes a function of the velocity gradient causing the hydrodynamic orientation. These general ideas are applied to various species of molecules and particles. For the small rigid particle view, in laminar flow the anisotropic particles are compelled to rotate with a nonuniform angular velocity. In more complicated systems, the hydrodynamic forces may induce structural orientations and modifications.

(e) Integrated Optical Effect for a Cylinder or an Edge

Assume that the stress-optic relations for solids are directly applicable to fluids. The integrated optical effects as encountered with an oscillating cylinder or at the edge of an oscillating plane may then be dealt with as follows. Consider the sections A-A and B-B normal to the light path as shown in figure 18. The plane is oscillating into and out of the plane of the page.

In section A-A, the principal stresses are oriented as shown in figure 18. For a given light path, the directions and magnitudes of these principal stresses are constant, depending on the distance from the oscillating plane, in all sections parallel to section A-A and lying between the extremes of the oscillating plane. Within the interval, the fringe order is given by equation (B.1).

For treating a section such as section B-B in figure 18, assume that the flow laminae curve around the edges of the plane as they do for an oscillating cylinder. Then, since the distance cd is greater than the distance ab, the magnitude of the secondary principal stresses in section

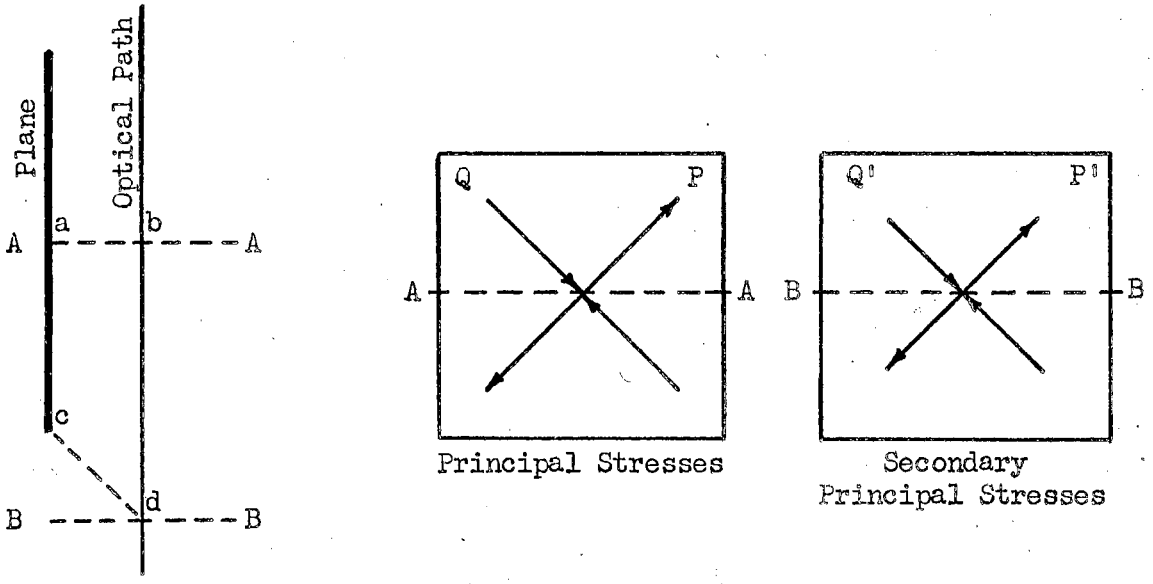

Figure 18. Principal stresses and secondary principal stresses in typical sections normal to the light path for an oscillating plane.

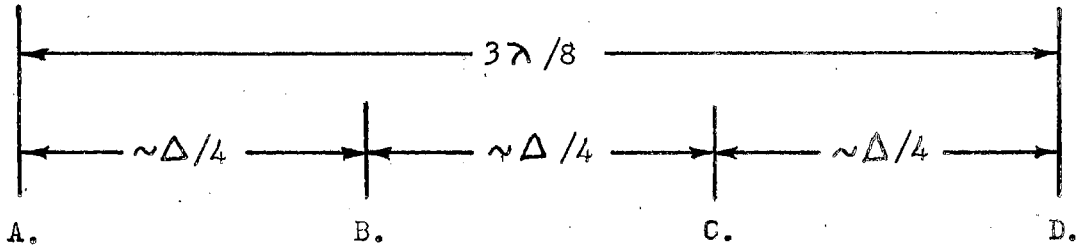

A. Surface of Oscillating Plane or Cylinder

B. Observed Zero Order Fringe for an Oscillating Cylinder

C. Observed Zero Order Fringe for an Oscillating Plane

D. Theoretical Zero Order Fringe in a Thin Mid-Section of the Fluid for an Oscillating Cylinder or Plane

Figure 19. Summary of results showing the relative positions of observed and theoretical zero order fringes for oscillating cylinders and planes when the surface velocity is positive maximum.

B-B will in general be different from the magnitudes of the principal stresses in section A-A. The orientations will be the same. Thus, beyond the edges of the oscillating plane, the fringe order will be given by equation (B.2), where the integration is made over the portions of the light path lying beyond the plane laminar region.

To get an expression for the resultant fringe order, combine equations (B.1) and (B.2). The expression is

$$n = C(P-Q)T + C\int_{path}(P'-Q')dT. \qquad (B.3)$$

For a zero order fringe to result requires that $n = 0$ or

$$(P-Q)T + \int_{path}(P'-Q')dT = 0 \qquad (B.4)$$

rather than simply $(P-Q) = 0$ where the end effects are neglected.

Experimental and theoretical results are summarized in figure 19. These show that for the oscillating plane, the shift in position of an observed zero order fringe from its theoretical position is in the same direction as the shift observed for an oscillating cylinder. These observations support the concept of zero order fringe shift due to optical end effects.

VITA

Logan E. Hargrove, Jr.

Candidate for the Degree of

Master of Science

Thesis: OPTICAL BIREFRINGENCE INDUCED BY SHEAR WAVE PROPAGATION IN AQUEOUS MILLING YELLOW SOLUTIONS

Major Field: Physics

Biographical:

Personal data: Born in Spiro, Oklahoma, March 3, 1935, the son of Logan E. and Ila Mae Hargrove.

Education: Attended grade school in Stillwater, Oklahoma; graduated from Stillwater High School in 1952; received the Bachelor of Science degree from the Oklahoma Agricultural and Mechanical College, with a major in Physics, in May, 1956; completed the requirements for the Master of Science degree in August, 1957.

Professional experience: Worked as a Research Assistant in the Department of Physics, from September, 1954, through May, 1957, on "Research in Nonlinear Properties of Fluid Flow Through Circular Orifices", supported by the Office of Ordnance Research of the United States Army and by the Research Foundation of the Oklahoma Agricultural and Mechanical College; a part of this research is described in this thesis.

Professional and honorary organizations: Associate member of the Acoustical Society of America and the Society of the Sigma Xi; member of Omicron Delta Kappa Honorary Leadership Society for Men, Sigma Pi Sigma Honorary Physics Society, Kappa Kappa Psi Honorary Bandsmen's Fraternity, and Phi Eta Sigma Freshman Honor Fraternity.